An adaptive stabilized finite element method for the Darcy's equations with pressure dependent viscosities

Araya, Rodolfo; Cárcamo, Cristian; Poza, Abner H.

Published in:
Computer Methods in Applied Mechanics and Engineering

DOI:
10.1016/j.cma.2021.114100

Available online at www.sciencedirect.com
ScienceDirect
Comput. Methods Appl. Mech. Engrg. 387 (2021) 114100
Computer methods in applied mechanics and engineering
www.elsevier.com/locate/cma

An adaptive stabilized finite element method for the Darcy's equations with pressure dependent viscosities

Rodolfo Araya[a], Cristian Cárcamo[a,c,*], Abner H. Poza[b]

[a] Departamento de Ingeniería Matemática & CI^2MA, Universidad de Concepción, Casilla 160-C, Concepción, Chile
[b] Departamento de Matemática y Física Aplicadas, Universidad Católica de la Santísima Concepción, Casilla 297, Concepción, Chile
[c] Bernoulli Institute, University of Groningen, 9747 AG, Groningen, The Netherlands

Received 13 November 2020; received in revised form 2 August 2021; accepted 8 August 2021
Available online 13 September 2021

Abstract

This work aims to introduce and analyze an adaptive stabilized finite element method to solve a nonlinear Darcy equation with a pressure-dependent viscosity and mixed boundary conditions. We stated the discrete problem's well-posedness and optimal error estimates, in natural norms, under standard assumptions. Next, we introduce and analyze a residual-based a posteriori error estimator for the stabilized scheme. Finally, we present some two- and three-dimensional numerical examples which confirm our theoretical results.

Keywords: Nonlinear Darcy's equation; Stabilized finite element method; a priori error analysis; a posteriori error analysis

1. Introduction

In many critical applications, it becomes necessary to study the fluids flow through a porous medium, such as in oil reservoirs, contaminant transport, mesoscale blood flows, filter design, and water resource problems. The first model adopted to study this phenomenon corresponds to the Darcy model (see [1]) when the fluid viscosity is considered to be a constant and the pressure is independent of this viscosity. Then it was proved experimentally that in a wide variety of industrial applications, as in the case of organic liquid, viscosity can be pressure-dependent (see [2]). This situation occurs, for example, when the viscosity has an exponential dependence on pressure (see [2]), turning the Darcy problem into a nonlinear problem (for details on the derivation, see [3]).

For the classical Darcy equation, there are a large number of numerical schemes that approximate the velocity and pressure of the fluid, including some mixed methods that consider the stable subspace of $H(\mathrm{div};\Omega)$, such as the Raviart–Thomas [4] or Brezzi–Douglas–Marini elements [5]. For an incomplete list of these stable schemes, see [6–11] and the references therein.

On the other hand, in fluid dynamics simulations, the usage of equal-order interpolation subspaces for pressure and velocity is a desirable property. However, this choice, unfortunately, does not lead to stable finite element methods that fulfill the Babuska–Brezzi–Ladyzenskaya condition (see [12] and the references therein). In order to overcome this problem, several stabilized finite-element methods have been proposed over the last decades.

* Corresponding author.
E-mail addresses: rodolfo.araya@udec.cl (R. Araya), c.e.carcamo@rug.nl (C. Cárcamo), apoza@ucsc.cl (A.H. Poza).

https://doi.org/10.1016/j.cma.2021.114100

Some remarkable examples of stabilized methods, which add residual terms to the Galerkin formulation, consist of the SUPG/PSPG or SDFEM methods (see, for instance, [13–16]). A minor variation of these schemes is the so-called Residual Local Projection (RELP) methods, which reintroduce the residues through interpolation operators (fluctuation operators) on finite-dimensional spaces using the solution of local problems (see, for example, [17] for the Stokes equations, [18] for the Darcy equations, and [19] for the Navier–Stokes equations). When the additional terms are not residual-based, the Orthogonal Subscales method (see [20]), the CIP methods (see [21]), or the Local Projection Stabilization (LPS) method (see [22]) can be employed. The LPS methods can also be considered as a simplification of the RELP method. This method considers symmetric term-by-term fluctuation terms, therefore generating a method that, although simpler, lacks a consistency property (see, for instance, [23] for the Oseen equations and [24] for the Navier–Stokes equations). Another list of stabilized schemes for the linear Darcy equation is [25–30]. A different strategy to approach this problem consists of multilevel approximation, such as the Multiscale Hybrid-Mixed (MHM) method (for details, see [31,32]).

Regarding the nonlinear Darcy equation, the list of numerical schemes is relatively short when, for instance, the viscosity is pressure-dependent. In [33], an approximation of the nonlinear equation in a circular well-established domain using a spectral element discretization was proposed and analyzed. In [34], this strategy was extended to consider an a posteriori error estimator so as to improve the performance of a simplified model in which pressure dependence does not show much variation. In [35], the authors used the implicit Euler scheme to extend the spectral element discretization to the non-stationary case. A study of the convergence of a stable finite element discretization can be found in [36] for the nonlinear problem when the viscosity dependence on pressure is a bounded function. A mixed finite element method with a Lagrange multiplier was introduced and analyzed in [37] for stable subspaces. The authors also introduced an a posteriori error estimator to enhance the quality of the results. Extending the ideas presented in [25], a stabilized finite element method was proposed in [16] when the viscosity dependence on pressure can occur in several different ways. A scalable numerical formulation based on variational inequalities was recently presented in [38], and the convergence of the last two schemes mentioned was carried out in a numerical form.

This work aims to present and analyze a stabilized finite element method for the nonlinear Darcy equations when the viscosity can be exponentially dependent on pressure, for example, when this dependency satisfies the Barus law [39]. As in [37], we use a change of variable that allows us to transform the nonlinear equation into a linear problem. Implementing the ideas of [25], a new stabilized finite element method was defined. This new scheme is free of mesh-dependent stabilization parameters and allows the classical $\mathbb{P}_k^d \times \mathbb{P}_k$ elements for velocity and pressure. To ensure the method's stability, some tools presented in [37] were used, such as the Banach fixed point theorem and a generalized Lax–Milgram theorem. In the convergence analysis, we employed strategies from the analysis of other classical stabilized finite element method (for details, see [40,41]). Thus, our contribution corresponds to the numerical analysis of the discrete scheme, as well as the definition of a residual-based a posteriori error estimator.

This work is organized as follows: In Section 2 the nonlinear Darcy equation and the variational formulation of the linear problem obtained from a change of variable is introduced. Some preliminary results that will be needed later are presented at the end of this section. In Section 3, we described the stabilized finite element approximation proposed and included the well-posedness of the scheme. This section also includes a priori error estimates for the elements $\mathbb{P}_k^d \times \mathbb{P}_k$.

Then, an a posteriori error estimator related to the new stabilized scheme is presented and analyzed in Section 4. We also showed the equivalence between the error estimator and the approximation error in natural norms. In Section 5, we presented the adaptive procedure established, in addition to the numerical results that validate the a priori error results and the performance of the a posteriori error estimator. Finally, in Appendix A, we proved a technical result essential for our adaptive scheme.

2. Model problem and preliminary results

Let Ω be a bounded domain in $\mathbb{R}^d$, $d = 2, 3$ with polygonal boundary $\partial\Omega$ divided in Γ_D and Γ_N, with $\Gamma_D \cap \Gamma_N = \emptyset$ and $\Gamma_D \neq \emptyset$. We focus in to seek the velocity and pressure solution $(\tilde{\boldsymbol{u}}, \tilde{p})$ to the nonlinear Darcy equations, with mixed boundary condition, given by:

$$\begin{cases} \alpha(\tilde{p})\tilde{\boldsymbol{u}} + \nabla\tilde{p} &= \boldsymbol{f} \quad \text{in } \Omega, \\ \nabla\cdot\tilde{\boldsymbol{u}} &= 0 \quad \text{in } \Omega, \\ \tilde{p} &= \tilde{\varphi} \quad \text{on } \Gamma_D, \\ \tilde{\boldsymbol{u}}\cdot\boldsymbol{n} &= 0 \quad \text{on } \Gamma_N, \end{cases} \tag{2.1}$$

where $\alpha(\tilde{p})$ is the drag function, $\tilde{\varphi} \in H^{1/2}(\Gamma_D)$ is the prescribed pressure in $\Gamma_D, \boldsymbol{f} \in L^2(\Omega)^d$ is a given source and $\boldsymbol{n}$ is the unit outward normal vector to $\partial\Omega$.

Remark 1. When $\Gamma_N = \partial\Omega$ it is necessary, for the uniqueness of the solution, to impose the condition $\int_\Omega \tilde{p} = 0$. In this work, we consider $|\Gamma_D| > 0$, which is more complex to analyze.

In the standard Darcy equation, the drag coefficient α is equal to the ratio of the viscosity μ of the fluid and the permeability κ of the porous media, i.e.

$$\alpha = \frac{\mu}{\kappa}. \tag{2.2}$$

In this work, we follow Barus [39], who proposed the exponential dependence of viscosity on pressure given by the function

$$\mu(s) = \mu_0 e^{\gamma s}, \quad \forall s \in \mathbb{R}, \tag{2.3}$$

where μ_0 is a positive constant and γ is called the Barus coefficient, which can be obtained experimentally (see [2]). Thereby, from (2.2) and (2.3) we get

$$\alpha(s) = \alpha_0 e^{\gamma s}, \quad \forall s \in \mathbb{R}, \tag{2.4}$$

where $\alpha_0 := \dfrac{\mu_0}{\kappa}$.

Now, thanks to the (2.4) and in view of analysis, we will rewrite the problem (2.1) in a more convenient form. To this end, the first equality of (2.1) is reduced to

$$\tilde{\boldsymbol{u}} = \frac{1}{\alpha(\tilde{p})}(\boldsymbol{f} - \nabla\tilde{p}) = \frac{1}{\alpha_0} e^{-\gamma\tilde{p}} \boldsymbol{f} + \frac{1}{\alpha_0\gamma}\nabla(e^{-\gamma\tilde{p}}).$$

Now, defining $\boldsymbol{u} := \tilde{\boldsymbol{u}}$, and $p := e^{-\gamma\tilde{p}} - 1$, and using (2.1), we define the following Darcy equation

$$\begin{cases} \boldsymbol{u} &= \dfrac{1}{\alpha_0}(p+1)\boldsymbol{f} + \dfrac{1}{\varepsilon}\nabla p & \text{in } \Omega, \\ \nabla\cdot\boldsymbol{u} &= 0 & \text{in } \Omega, \\ p &= \varphi & \text{on } \Gamma_D, \\ \boldsymbol{u}\cdot\boldsymbol{n} &= 0 & \text{on } \Gamma_N, \end{cases} \tag{2.5}$$

where $\varepsilon := \alpha_0\gamma > 0$ and $\varphi := e^{-\gamma\tilde{\varphi}} - 1$. This transformation was introduced in [37], where the authors present a similar mixed variational formulation for (2.5), with different Hilbert spaces and using a Lagrange multiplier to weakly impose some boundary conditions.

In the sequel we will use the following Hilbert spaces,

$$\boldsymbol{H} := \{\boldsymbol{v} \in H(\text{div}; \Omega) : \boldsymbol{v}\cdot\boldsymbol{n} = 0 \text{ on } \Gamma_N\},$$
$$\tilde{Q} := L^2(\Omega),$$

and the norms

$$\|\boldsymbol{v}\|_{\boldsymbol{H}} = \|\boldsymbol{v}\|_{\text{div};\Omega} \qquad \text{and} \qquad \|q\|_{\tilde{Q}} = \|q\|_{0,\Omega},$$

for all $\boldsymbol{v} \in \boldsymbol{H}$ and $q \in \tilde{Q}$.

The variational formulation of problem (2.5) can be written as: *Find* $(\boldsymbol{u}, p) \in \boldsymbol{H} \times \tilde{Q}$ *such that*

$$a(\boldsymbol{u}, \boldsymbol{v}) + b(\boldsymbol{v}, p) = \langle \boldsymbol{v}\cdot\boldsymbol{n}, \varphi\rangle_{\Gamma_D} + \gamma\,(p\boldsymbol{f}, \boldsymbol{v}) + \gamma\,(\boldsymbol{f}, \boldsymbol{v}) \qquad \forall \boldsymbol{v} \in \boldsymbol{H}, \tag{2.6}$$

$$b(\boldsymbol{u}, q) = 0 \qquad \forall q \in \tilde{Q}, \tag{2.7}$$

where $a : \boldsymbol{H} \times \boldsymbol{H} \longrightarrow \mathbb{R}$ and $b : \boldsymbol{H} \times \tilde{Q} \longrightarrow \mathbb{R}$ are the bilinear forms defined by

$$a(\boldsymbol{u}, \boldsymbol{v}) := \varepsilon\,(\boldsymbol{u}, \boldsymbol{v}) \qquad \forall (\boldsymbol{u}, \boldsymbol{v}) \in \boldsymbol{H} \times \boldsymbol{H}, \tag{2.8}$$

$$b(\boldsymbol{v}, q) := (q, \nabla\cdot\boldsymbol{v}) \qquad \forall (\boldsymbol{v}, q) \in \boldsymbol{H} \times \tilde{Q}. \tag{2.9}$$

Here $(\cdot,\cdot)$ stands for the $L^2(\Omega)$-inner product, where we use the same notation for vector, or tensor, valued functions, and $\langle\cdot,\cdot\rangle_{\Gamma_D}$ is the duality pairing between $H^{-1/2}(\Gamma_D)$ and $H^{1/2}(\Gamma_D)$.

Also we consider the norm, on $H^{-1/2}(\Gamma_D)$, given by

$$\|\mu\|_{-1/2,\Gamma_D} := \inf_{\substack{\sigma\in H(\mathrm{div};\,\Omega)\\ \sigma\cdot n=\mu \text{ on } \Gamma_D}} \|\boldsymbol{\sigma}\|_{\boldsymbol{H}}, \tag{2.10}$$

for all $\mu \in H^{-1/2}(\Gamma_D)$.

We equip the space $\boldsymbol{H} \times \tilde{Q}$ with the product norm

$$\|(\boldsymbol{w}, r)\|_{\boldsymbol{H}\times\tilde{Q}} = \|\boldsymbol{w}\|_{\boldsymbol{H}} + \|r\|_{0,\Omega}.$$

Throughout this paper C and C_i, $i > 0$ will denote positive constants independent of the mesh size h, but who may depend on the parameter ε.

The next result states some inequalities which will be used in the sequel.

Lemma 1. *Let $a(\cdot,\cdot)$ and $b(\cdot,\cdot)$ be the bilinear forms given by* (2.8) and (2.9), *respectively. Then, there exists a positive constant β_b, such that*

$$|a(\boldsymbol{u},\boldsymbol{v})| \le \varepsilon\|\boldsymbol{u}\|_{\boldsymbol{H}}\|\boldsymbol{v}\|_{\boldsymbol{H}} \qquad \forall\, \boldsymbol{u},\boldsymbol{v} \in \boldsymbol{H}, \tag{2.11}$$

$$|b(\boldsymbol{v},q)| \le \|q\|_{\tilde{Q}}\|\boldsymbol{v}\|_{\boldsymbol{H}} \qquad \forall\, \boldsymbol{v} \in \boldsymbol{H},\ \forall q \in \tilde{Q}, \tag{2.12}$$

$$\sup_{\boldsymbol{v}\in\boldsymbol{H}} \frac{b(\boldsymbol{v},q)}{\|\boldsymbol{v}\|_{\boldsymbol{H}}} \ge \beta_b\,\|q\|_{\tilde{Q}} \qquad \forall q \in \tilde{Q}. \tag{2.13}$$

Proof. The proof of (2.11) and (2.12) follows from norm definitions. For (2.13) see [42, (7.1.13)]. □

The next result guarantees the solvability of problem (2.6)–(2.7).

Theorem 2. *Assume that $\boldsymbol{f} \in L^\infty(\Omega)^d$ and*

$$\left(\frac{1}{\varepsilon} + \frac{2}{\beta_b}\right)\gamma\,\|\boldsymbol{f}\|_{\infty,\Omega} < 1. \tag{2.14}$$

Then, problem (2.6)–(2.7) *has a unique solution $(\boldsymbol{u}, p) \in \boldsymbol{H} \times \tilde{Q}$ and there exist a positive constant C, independent of ε and γ, such that*

$$\|(\boldsymbol{u}, p)\|_{\boldsymbol{H}\times\tilde{Q}} \le C\left(\frac{1}{\varepsilon} + \frac{2}{\beta_b}\right)\|\boldsymbol{f}\|_{\infty,\Omega}. \tag{2.15}$$

Proof. The proof is a simple adaptation of [37, Theorem 3.1]. □

In the rest of this work, we find the pressure solution $p \in Q := H^1(\Omega)$, and over $\boldsymbol{H} \times Q$ we will define the following norm

$$|||(\boldsymbol{w}, r)||| := \varepsilon^{1/2}\,\|\boldsymbol{w}\|_{\boldsymbol{H}} + \|r\|_{1,\Omega},$$

for all $(\boldsymbol{w}, r) \in \boldsymbol{H} \times Q$.

3. The stabilized finite element method

From now on, we denote by $\{\mathcal{T}_h\}_{h>0}$ a regular family of triangulations of $\bar{\Omega}$ composed by simplexes. For a $\mathcal{T}_h$ we will denote by T the elements of the triangulation, and by $\mathcal{E}_h$ the set of all edges (faces) of $\mathcal{T}_h$, with the splitting $\mathcal{E}_h = \mathcal{E}_\Omega \cup \mathcal{E}_D \cup \mathcal{E}_N$, where $\mathcal{E}_\Omega$ stands for the edges (faces) lying in the interior of Ω, $\mathcal{E}_D$ and $\mathcal{E}_N$ stands for the edges (faces) on the boundaries Γ_D and Γ_N, respectively. As usual h_T means the diameter of T, $h = \max_{T\in\mathcal{T}_h} h_T$, and $h_F := |F|$ for $F \in \mathcal{E}_h$.

We introduce two finite element subspaces of $\boldsymbol{H}$ and Q, given by

$$\boldsymbol{H}_h := \{\boldsymbol{v} \in C(\overline{\Omega})^d \ :\ \boldsymbol{v}|_T \in \mathbb{P}_k(T)^d, \quad \forall T \in \mathcal{T}_h\} \cap \boldsymbol{H},$$

$$Q_h := \{q \in C(\overline{\Omega}) \ :\ q|_T \in \mathbb{P}_k(T), \quad \forall T \in \mathcal{T}_h\},$$

with $k \ge 1$, where $\mathbb{P}_k$ stands for the space of polynomials of total degree less or equal to k.

Next, we consider the following discrete stabilized scheme: *Find* $(\boldsymbol{u}_h, p_h) \in \boldsymbol{H}_h \times Q_h$ such that

$$B_{\text{stab}}((\boldsymbol{u}_h, p_h), (\boldsymbol{v}_h, q_h)) = \langle \boldsymbol{v}_h \cdot \boldsymbol{n}, \varphi\rangle_{\Gamma_D} + \gamma((p_h + 1)\boldsymbol{f}, \boldsymbol{v}_h) - \frac{1}{2}\left(\varepsilon^{-1}\,\gamma\,(p_h + 1)\boldsymbol{f}, \varepsilon\boldsymbol{v}_h + \nabla q_h\right), \tag{3.1}$$

for all $(\boldsymbol{v}_h, q_h) \in \boldsymbol{H}_h \times Q_h$, where

$$B_{\text{stab}}((\boldsymbol{w}_h, r_h), (\boldsymbol{v}_h, q_h)) := a(\boldsymbol{w}_h, \boldsymbol{v}_h) + b(\boldsymbol{v}, r_h) - b(\boldsymbol{w}_h, q_h) - \frac{1}{2}\left(\varepsilon^{-1}(\varepsilon\boldsymbol{w}_h - \nabla r_h), \varepsilon\,\boldsymbol{v}_h + \nabla q_h\right) + \varepsilon\,(\nabla\cdot\boldsymbol{w}_h, \nabla\cdot\boldsymbol{v}_h). \tag{3.2}$$

Remark 2. This scheme, as well as the proposed in [16], is based on the stabilized finite element method, for the linear Darcy equation, presented in [25], with the difference that in our scheme we add an $\varepsilon\,(\nabla\cdot\boldsymbol{u}_h, \nabla\cdot\boldsymbol{v}_h)$ term which improves the quality of the numerical results.

The following result will be fundamental to prove the well-posedness of the stabilized finite element scheme. The proof is based on the same arguments used in [41, Lemma 4.1].

Lemma 3. *Let $B_{\text{stab}}(\cdot,\cdot)$ be the bilinear form defined in (3.2). Then there is a positive constant β_s, independent of h and ε, such that*

$$\sup_{(\boldsymbol{v}_h,q_h)\in\boldsymbol{H}_h\times Q_h} \frac{B_{\text{stab}}((\boldsymbol{u}_h, p_h), (\boldsymbol{v}_h, q_h))}{|||(\boldsymbol{v}_h, q_h)|||} \geq \beta_s\,|||(\boldsymbol{u}_h, p_h)|||, \tag{3.3}$$

for all $(\boldsymbol{u}_h, p_h) \in \boldsymbol{H}_h \times Q_h$.

Proof. Let $(\boldsymbol{u}_h, p_h) \in \boldsymbol{H}_h \times Q_h$ and let $\boldsymbol{w}_h \in \boldsymbol{H}_h$ be a function for which the supremum in Lemma 10 is attained, and such that $\|\boldsymbol{w}_h\|_{\boldsymbol{H}} = \|p_h\|_{0,\Omega}$. If we consider $\tilde{\boldsymbol{w}}_h = -\boldsymbol{w}_h$, we have

$$\frac{-(p_h, \nabla\cdot\tilde{\boldsymbol{w}}_h)}{\|\tilde{\boldsymbol{w}}_h\|_{\boldsymbol{H}}} = \frac{(p_h, \nabla\cdot\boldsymbol{w}_h)}{\|\boldsymbol{w}_h\|_{\boldsymbol{H}}} \geq \beta_w\|p_h\|_{0,\Omega} - \lambda|p_h|_{1,\Omega},$$

and therefore,

$$-\,(p_h, \nabla\cdot\tilde{\boldsymbol{w}}_h) \geq \beta_w\|p_h\|^2_{0,\Omega} - \lambda|p_h|_{1,\Omega}\|\tilde{\boldsymbol{w}}_h\|_{\boldsymbol{H}}. \tag{3.4}$$

Then, for $(\boldsymbol{v}_h, q_h) := (\boldsymbol{u}_h - \delta\tilde{\boldsymbol{w}}_h, p_h)$, with $\delta > 0$, we get that

$$\begin{aligned}
B_{\text{stab}}((\boldsymbol{u}_h, p_h), (\boldsymbol{v}_h, q_h)) =& B_{\text{stab}}((\boldsymbol{u}_h, p_h), (\boldsymbol{u}_h, p_h)) - \delta\,B_{\text{stab}}((\boldsymbol{u}_h, p_h), (\tilde{\boldsymbol{w}}_h, 0)) \\
=& B_{\text{stab}}((\boldsymbol{u}_h, p_h), (\boldsymbol{u}_h, p_h)) - \delta\left[B_{\text{stab}}((\boldsymbol{u}_h, 0), (\tilde{\boldsymbol{w}}_h, 0)) + B_{\text{stab}}((\boldsymbol{0}, p_h), (\tilde{\boldsymbol{w}}_h, 0))\right] \\
=& \frac{1}{2}\varepsilon\,\|\boldsymbol{u}_h\|^2_{0,\Omega} + \varepsilon\,\|\nabla\cdot\boldsymbol{u}_h\|^2_{0,\Omega} + \frac{1}{2}\varepsilon^{-1}\,|p_h|^2_{1,\Omega} \\
&- \delta\left[\frac{1}{2}\varepsilon\,(\boldsymbol{u}_h, \tilde{\boldsymbol{w}}_h) + \varepsilon\,(\nabla\cdot\boldsymbol{u}_h, \nabla\cdot\tilde{\boldsymbol{w}}_h) + (p_h, \nabla\cdot\tilde{\boldsymbol{w}}_h) + \frac{1}{2}\,(\nabla p_h, \tilde{\boldsymbol{w}}_h)\right] \\
=& \frac{1}{2}\varepsilon\,\|\boldsymbol{u}_h\|^2_{0,\Omega} + \varepsilon\,\|\nabla\cdot\boldsymbol{u}_h\|^2_{0,\Omega} + \frac{1}{2}\varepsilon^{-1}\,|p_h|^2_{1,\Omega} \\
&- \frac{\delta}{2}\varepsilon\,(\boldsymbol{u}_h, \tilde{\boldsymbol{w}}_h) - \delta\varepsilon\,(\nabla\cdot\boldsymbol{u}_h, \nabla\cdot\tilde{\boldsymbol{w}}_h) - \delta\,(p_h, \nabla\cdot\tilde{\boldsymbol{w}}_h) - \frac{\delta}{2}\,(\nabla p_h, \tilde{\boldsymbol{w}}_h) \\
\geq& \frac{1}{2}\varepsilon\,\|\boldsymbol{u}_h\|^2_{0,\Omega} + \varepsilon\,\|\nabla\cdot\boldsymbol{u}_h\|^2_{0,\Omega} + \frac{1}{2}\varepsilon^{-1}\,|p_h|^2_{1,\Omega} + \delta\beta_w\,\|p_h\|^2_{0,\Omega} - \delta\lambda|p_h|_{1,\Omega}\,\|\tilde{\boldsymbol{w}}_h\|_{\boldsymbol{H}} \\
&- \frac{\delta}{2}\varepsilon\,(\boldsymbol{u}_h, \tilde{\boldsymbol{w}}_h) - \delta\varepsilon\,(\nabla\cdot\boldsymbol{u}_h, \nabla\cdot\tilde{\boldsymbol{w}}_h) - \frac{\delta}{2}\,(\nabla p_h, \tilde{\boldsymbol{w}}_h) \\
\geq& \frac{1}{2}\varepsilon\,\|\boldsymbol{u}_h\|^2_{0,\Omega} + \varepsilon\,\|\nabla\cdot\boldsymbol{u}_h\|^2_{0,\Omega} + \frac{1}{2}\varepsilon^{-1}\,|p_h|^2_{1,\Omega} + \delta\beta_w\,\|p_h\|^2_{0,\Omega} \\
&- \frac{\delta}{2}\varepsilon\,\|\boldsymbol{u}_h\|_{0,\Omega}\|\tilde{\boldsymbol{w}}_h\|_{0,\Omega} - \delta\varepsilon\,\|\nabla\cdot\boldsymbol{u}_h\|_{0,\Omega}\|\nabla\cdot\tilde{\boldsymbol{w}}_h\|_{0,\Omega} \\
&- \frac{\delta}{2}|p_h|_{1,\Omega}\|\tilde{\boldsymbol{w}}_h\|_{0,\Omega} - \delta\lambda|p_h|_{1,\Omega}\|\tilde{\boldsymbol{w}}_h\|_{\boldsymbol{H}}.
\end{aligned}$$

Now, using Young's inequality $2ab \leq \dfrac{a^2}{\gamma} + \gamma\, b^2$, for all $a, b, \gamma > 0$, and the fact that $\|\tilde{\boldsymbol{w}}_h\|_{\boldsymbol{H}} = \|p_h\|_{0,\Omega}$, we get

$$
\begin{aligned}
B_{\text{stab}}((\boldsymbol{u}_h, p_h), (\boldsymbol{v}_h, q_h)) \geq & \frac{1}{2}\varepsilon\, \|\boldsymbol{u}_h\|^2_{0,\Omega} + \varepsilon\, \|\nabla\cdot\boldsymbol{u}_h\|^2_{0,\Omega} + \frac{1}{2}\varepsilon^{-1}\, |p_h|^2_{1,\Omega} + \delta\beta_w\, \|p_h\|^2_{0,\Omega} \\
& - \frac{\delta\varepsilon}{4\gamma_1}\, \|\boldsymbol{u}_h\|^2_{0,\Omega} - \frac{\delta\varepsilon\gamma_1}{4}\, \|\tilde{\boldsymbol{w}}_h\|^2_{0,\Omega} \\
& - \frac{\delta\varepsilon}{2\gamma_2}\, \|\nabla\cdot\boldsymbol{u}_h\|^2_{0,\Omega} - \frac{\delta\varepsilon\gamma_2}{2}\, \|\nabla\cdot\tilde{\boldsymbol{w}}_h\|^2_{0,\Omega} \\
& - \frac{\delta}{4\gamma_3}|p_h|^2_{1,\Omega} - \frac{\delta\gamma_3}{4}\|\tilde{\boldsymbol{w}}_h\|^2_{0,\Omega} \\
& - \frac{\delta\lambda}{2\gamma_4}|p_h|^2_{1,\Omega} - \frac{\delta\lambda\gamma_4}{2}\|\tilde{\boldsymbol{w}}_h\|^2_{\boldsymbol{H}} \\
\geq & \frac{1}{2}\varepsilon\left(1 - \frac{\delta}{2\gamma_1}\right)\|\boldsymbol{u}_h\|^2_{0,\Omega} + \varepsilon\left(1 - \frac{\delta}{2\gamma_2}\right)\|\nabla\cdot\boldsymbol{u}_h\|^2_{0,\Omega} \\
& + \frac{1}{2}\left(\varepsilon^{-1} - \frac{\delta}{2\gamma_3} - \frac{\delta\lambda}{2\gamma_4}\right)|p_h|^2_{1,\Omega} \\
& + \delta\left(\beta_w - \frac{\delta\varepsilon\gamma_1}{4} - \frac{\delta\varepsilon\gamma_2}{2} - \frac{\delta\gamma_3}{4} - \frac{\delta\lambda\gamma_4}{2}\right)\|p_h\|^2_{0,\Omega} \\
\geq & \frac{1}{2}\varepsilon\left(1 - \frac{\delta}{2\gamma_1}\right)\|\boldsymbol{u}_h\|^2_{0,\Omega} + \varepsilon\left(1 - \frac{\delta}{2\gamma_2}\right)\|\nabla\cdot\boldsymbol{u}_h\|^2_{0,\Omega} \\
& + \frac{1}{2}\left(\varepsilon^{-1} - \frac{\delta}{2\gamma_3} - \frac{\delta\lambda}{2\gamma_4}\right)|p_h|^2_{1,\Omega} + \delta C_{10}\,\|p_h\|^2_{0,\Omega},
\end{aligned}
$$

with $C_{10} > 0$, if γ_1, γ_2, γ_3 and γ_4 are chosen small enough.

Now, if we choose $0 < \delta < \min\left\{2\gamma_1, 2\gamma_2, \dfrac{2\gamma_3\gamma_4\varepsilon^{-1}}{\gamma_4 + \gamma_3\lambda}, \varepsilon^{-1/2}\right\}$, we have

$$B_{\text{stab}}((\boldsymbol{u}_h, p_h), (\boldsymbol{v}_h, q_h)) \geq C\, |||(\boldsymbol{u}_h, p_h)|||^2. \tag{3.5}$$

On the other hand, using the definition of $\boldsymbol{v}_h, q_h, \delta$ and the triangle inequality, we have

$$|||(\boldsymbol{v}_h, q_h)||| \leq \sqrt{\varepsilon}\, \|\boldsymbol{u}_h\|_{\boldsymbol{H}} + \delta\sqrt{\varepsilon}\, \|p_h\|_{0,\Omega} + \|p_h\|_{1,\Omega} \leq C\, |||(\boldsymbol{u}_h, p_h)|||,$$

thus, using (3.5), we complete the proof. □

Remark 3. This result is also valid for the continuous spaces $\boldsymbol{H}$ and Q and it will be used in the analysis of the a posteriori error estimator proposed in Section 4 (for details, see Lemma 11). On the other hand, if we use stable subspaces of $\boldsymbol{H}$ and Q, as for example, Raviart–Thomas elements of degree k, for the velocity, and piecewise polynomial elements of order k, for the pressure, or the Brezzi–Douglas–Marini spaces of order k, for the velocity, and piecewise polynomial elements of order $k-1$, for the pressure, Lemma 3 is also true (for details on stable subspaces, see [42]). In both cases the proof is similar to that proposed for Lemma 11 and therefore (3.1) can be seen as an augmented finite element method when stable subspaces of $\boldsymbol{H}$ and Q are used.

Concerning the well-posedness of the stabilized discrete problem (3.1), we have the following result.

Theorem 4. *Let $\beta_s > 0$ as in (3.3) and $\beta_c > 0$ as in (A.7). If*

$$\gamma\, \|\boldsymbol{f}\|_{\infty,\Omega} \leq \frac{\min\{\beta_s, \beta_c\}\,\varepsilon^{1/2}}{3 + \varepsilon^{-1/2}}, \tag{3.6}$$

then the discrete stabilized problem (3.1) has a unique solution $(\boldsymbol{u}_h, p_h) \in \boldsymbol{H}_h \times Q_h$.

Proof. To prove the result, we write the solution of the problem (3.1), as the solution of a fixed point problem. Thereby, given $r \in L^2(\Omega)$, we define the linear functionals

$$\boldsymbol{F}^s_r : \boldsymbol{H}_h \times Q_h \longrightarrow \mathbb{R} \quad \text{and} \quad \boldsymbol{F}^s : \boldsymbol{H}_h \times Q_h \longrightarrow \mathbb{R},$$

by

$$\boldsymbol{F}^s_r(\boldsymbol{v}_h, q_h) := \gamma(r\boldsymbol{f}, \boldsymbol{v}_h) - \frac{1}{2}\big(\varepsilon^{-1}\gamma\, r\boldsymbol{f},\ \varepsilon\,\boldsymbol{v}_h + \nabla q_h\big),$$

$$\boldsymbol{F}^s(\boldsymbol{v}_h, q_h) := \langle \boldsymbol{v}_h \cdot \boldsymbol{n}, \varphi\rangle_{\Gamma_D} + \gamma(\boldsymbol{f}, \boldsymbol{v}_h) - \frac{1}{2}\big(\varepsilon^{-1}\gamma\boldsymbol{f},\ \varepsilon\,\boldsymbol{v}_h + \nabla q_h\big).$$

Now, we can write equation (3.1) as

$$B_{\mathrm{stab}}((\boldsymbol{u}_h, p_h), (\boldsymbol{v}_h, q_h)) = \boldsymbol{F}^s_{p_h}(\boldsymbol{v}_h, q_h) + \boldsymbol{F}^s(\boldsymbol{v}_h, q_h) \qquad \forall\, (\boldsymbol{v}_h, q_h) \in \boldsymbol{H}_h \times Q_h.$$

If we assume that $\boldsymbol{f} \in L^\infty(\Omega)^d$, the functional $\boldsymbol{F}^s_r$ satisfy

$$\begin{aligned} |\boldsymbol{F}^s_r(\boldsymbol{v}_h, q_h)| &\le \gamma\|r\|_{0,\Omega}\|\boldsymbol{f}\|_{\infty,\Omega}\|\boldsymbol{v}_h\|_{0,\Omega} + \frac{1}{2}\varepsilon^{-1}\gamma\|r\|_{0,\Omega}\|\boldsymbol{f}\|_{\infty,\Omega}\left\{\varepsilon\|\boldsymbol{v}_h\|_{0,\Omega} + \|\nabla q_h\|_{0,\Omega}\right\} \\ &\le \gamma\varepsilon^{-1/2}\|r\|_{0,\Omega}\|\boldsymbol{f}\|_{\infty,\Omega}|||(\boldsymbol{v}_h, q_h)||| + \frac{1}{2}\varepsilon^{-1}\gamma\|r\|_{0,\Omega}\|\boldsymbol{f}\|_{\infty,\Omega}\left\{\varepsilon^{1/2} + 1\right\}|||(\boldsymbol{v}_h, q_h)||| \\ &\le \frac{\varepsilon^{-1/2}}{2}\left\{3 + \varepsilon^{-1/2}\right\}\gamma\|r\|_{0,\Omega}\|\boldsymbol{f}\|_{\infty,\Omega}|||(\boldsymbol{v}_h, q_h)|||. \end{aligned} \tag{3.7}$$

Moreover, let $T_h : \boldsymbol{H}_h \times Q_h \longrightarrow \boldsymbol{H}_h \times Q_h$ the operator defined, for a given $(\boldsymbol{w}_h, r_h) \in \boldsymbol{H}_h \times Q_h$, by

$$T_h(\boldsymbol{w}_h, r_h) = (\bar{\boldsymbol{u}}_h, \bar{p}_h),$$

where $(\bar{\boldsymbol{u}}_h, \bar{p}_h) \in \boldsymbol{H}_h \times Q_h$ is the unique solution of the linear problem

$$B_{\mathrm{stab}}((\bar{\boldsymbol{u}}_h, \bar{p}_h), (\boldsymbol{v}_h, q_h)) = \boldsymbol{F}^s_{r_h}(\boldsymbol{v}_h, q_h) + \boldsymbol{F}^s(\boldsymbol{v}_h, q_h) \qquad \forall\, (\boldsymbol{v}_h, q_h) \in \boldsymbol{H}_h \times Q_h.$$

In this way, the discrete problem (3.1) can be written as follows: *Find* $(\boldsymbol{u}_h, p_h) \in \boldsymbol{H}_h \times Q_h$ *such that*

$$T_h(\boldsymbol{u}_h, p_h) = (\boldsymbol{u}_h, p_h).$$

Now, we can observe that

$$T_h(\boldsymbol{w}_h, r_h) = (\boldsymbol{u}^0_h, p^0_h) + S_h(\boldsymbol{w}_h, r_h) \qquad \forall\, (\boldsymbol{w}_h, r_h) \in \boldsymbol{H}_h \times Q_h,$$

where $(\boldsymbol{u}^0_h, p^0_h) \in \boldsymbol{H}_h \times Q_h$ is the unique solution of the auxiliar problem

$$B_{\mathrm{stab}}((\boldsymbol{u}^0_h, p^0_h), (\boldsymbol{v}_h, q_h)) = \boldsymbol{F}^s(\boldsymbol{v}_h, q_h), \qquad \forall\, (\boldsymbol{v}_h, q_h) \in \boldsymbol{H}_h \times Q_h, \tag{3.8}$$

and $S_h : \boldsymbol{H}_h \times Q_h \longrightarrow \boldsymbol{H}_h \times Q_h$ is the linear operator defined by

$$S_h(\boldsymbol{w}_h, r_h) = (\tilde{\boldsymbol{u}}_h, \tilde{p}_h)$$

where $(\tilde{\boldsymbol{u}}_h, \tilde{p}_h) \in \boldsymbol{H}_h \times Q_h$ satisfies the problem

$$B_{\mathrm{stab}}((\tilde{\boldsymbol{u}}_h, \tilde{p}_h), (\boldsymbol{v}_h, q_h)) = \boldsymbol{F}^s_{r_h}(\boldsymbol{v}_h, q_h), \qquad \forall\, (\boldsymbol{v}_h, q_h) \in \boldsymbol{H}_h \times Q_h. \tag{3.9}$$

Furthermore, using the continuous dependence result and inequality (3.7), we have that

$$|||S_h(\boldsymbol{w}_h, r_h)||| = |||(\tilde{\boldsymbol{u}}_h, \tilde{p}_h)||| \le \frac{\varepsilon^{-1/2}}{2\beta_s}\left\{3 + \varepsilon^{-1/2}\right\}\gamma\|r_h\|_{0,\Omega}\|\boldsymbol{f}\|_{\infty,\Omega}. \tag{3.10}$$

Let $(\boldsymbol{w}^1_h, r^1_h), (\boldsymbol{w}^2_h, r^2_h) \in \boldsymbol{H}_h \times Q_h$. Then, from (3.10) we have

$$\begin{aligned} |||T_h(\boldsymbol{w}^1_h, r^1_h) - T_h(\boldsymbol{w}^2_h, r^2_h)||| &= |||S_h(\boldsymbol{w}^1_h, r^1_h) - S_h(\boldsymbol{w}^2_h, r^2_h)||| \\ &= |||S_h(\boldsymbol{w}^1_h - \boldsymbol{w}^2_h, r^1_h - r^2_h)||| \\ &\le \frac{\varepsilon^{-1/2}}{2\beta_s}\left\{3 + \varepsilon^{-1/2}\right\}\gamma\|r^1_h - r^2_h\|_{0,\Omega}\|\boldsymbol{f}\|_{\infty,\Omega} \\ &\le \frac{\varepsilon^{-1/2}}{2\beta_s}\left\{3 + \varepsilon^{-1/2}\right\}\gamma\|\boldsymbol{f}\|_{\infty,\Omega}|||(\boldsymbol{w}^1_h - \boldsymbol{w}^2_h, r^1_h - r^2_h)|||. \end{aligned}$$

Thus, using condition (3.6), we have that

$$|||T_h(\boldsymbol{w}^1_h, r^1_h) - T_h(\boldsymbol{w}^2_h, r^2_h)||| \le \frac{1}{2}|||(\boldsymbol{w}^1_h - \boldsymbol{w}^2_h, r^1_h - r^2_h)|||.$$

The result follows using the Banach fixed point theorem. □

We consider the Lagrange interpolants $\boldsymbol{I}_h : H^{k+1}(\Omega)^d \longrightarrow \boldsymbol{H}_h$ and $\mathcal{J}_h : H^{k+1}(\Omega) \longrightarrow Q_h$ such that (see [43] for details):

$$|\boldsymbol{u} - \boldsymbol{I}_h\boldsymbol{u}|_{l,\Omega} \leq Ch^{s-l}\,|\boldsymbol{u}|_{s,\Omega}, \tag{3.11}$$

$$|p - \mathcal{J}_h p|_{l,\Omega} \leq Ch^{s-l}\,|p|_{s,\Omega}, \tag{3.12}$$

for all $\boldsymbol{u} \in H^s(\Omega)^d$ and all $p \in H^s(\Omega)$ with $l = 0, 1$ and $1 \leq s \leq k+1$.

Lemma 5. *Let $(\boldsymbol{u}, p)$ and $(\boldsymbol{u}_h, p_h)$ be the solutions of (2.5) and (3.1), respectively. If $(\boldsymbol{u}, p) \in H^{k+1}(\Omega)^d \cap \boldsymbol{H} \times H^{k+1}(\Omega)$, then it holds*

$$|B_{\text{stab}}((\boldsymbol{u}-\boldsymbol{u}_h, p-p_h), (\boldsymbol{v}_h, q_h))| \leq \frac{\varepsilon^{-1/2}}{2}(3+\varepsilon^{-1/2})\,\gamma\,\|\boldsymbol{f}\|_{\infty,\Omega}\|p-p_h\|_{0,\Omega}\,|||(\boldsymbol{v}_h, q_h)|||, \tag{3.13}$$

for all $(\boldsymbol{v}_h, q_h) \in \boldsymbol{H}_h \times Q_h$.

Proof. Using the regularity of the solution $(\boldsymbol{u}, p)$ of (2.5), we can prove that $\varepsilon\boldsymbol{u} - \gamma(p+1)\boldsymbol{f} - \nabla p = \boldsymbol{0}$, $\nabla\cdot\boldsymbol{u} = 0$ and $p = \varphi$ on Γ_D. Now, using integration by parts and the definition of $B_{\text{stab}}(\cdot,\cdot)$, we have

$$\begin{aligned}
B_{\text{stab}}((\boldsymbol{u}-\boldsymbol{u}_h, p-p_h), (\boldsymbol{v}_h, q_h)) &= B_{\text{stab}}((\boldsymbol{u}, p), (\boldsymbol{v}_h, q_h)) - B_{\text{stab}}((\boldsymbol{u}_h, p_h), (\boldsymbol{v}_h, q_h)) \\
&= \varepsilon(\boldsymbol{u}, \boldsymbol{v}_h) + (p, \nabla\cdot\boldsymbol{v}_h) - (q_h, \nabla\cdot\boldsymbol{u}) \\
&\quad - \frac{1}{2}\big(\varepsilon^{-1}(\varepsilon\boldsymbol{u} - \nabla p), \varepsilon\boldsymbol{v}_h + \nabla q_h\big) + \varepsilon\,(\nabla\cdot\boldsymbol{u}, \nabla\cdot\boldsymbol{v}_h) \\
&\quad - \langle\boldsymbol{v}_h\cdot\boldsymbol{n}, \varphi\rangle_{\Gamma_D} - \gamma((p_h+1)\boldsymbol{f}, \boldsymbol{v}_h) + \frac{1}{2}\big(\varepsilon^{-1}\gamma(p_h+1)\boldsymbol{f}, \varepsilon\boldsymbol{v}_h + \nabla q_h\big) \\
&= (\varepsilon\boldsymbol{u} - \gamma(p_h+1)\boldsymbol{f} - \nabla p, \boldsymbol{v}_h) \\
&\quad - \frac{1}{2}\big(\varepsilon^{-1}\big[\varepsilon\boldsymbol{u} - \nabla p - \gamma(p_h+1)\boldsymbol{f}\big], \varepsilon\boldsymbol{v}_h + \nabla q_h\big) \\
&= \big(\gamma(p-p_h)\boldsymbol{f}, \boldsymbol{v}_h\big) - \frac{1}{2}\big(\varepsilon^{-1}\gamma(p-p_h)\boldsymbol{f}, \varepsilon\boldsymbol{v}_h + \nabla q_h\big) \\
&= \frac{1}{2}\big(\gamma(p-p_h)\boldsymbol{f}, \boldsymbol{v}_h\big) - \frac{1}{2}\big(\varepsilon^{-1}\gamma(p-p_h)\boldsymbol{f}, \nabla q_h\big) \\
&\leq \frac{1}{2}\left\{\gamma\|p-p_h\|_{0,\Omega}\|\boldsymbol{f}\|_{\infty,\Omega}\varepsilon^{-1/2} + \gamma\|p-p_h\|_{0,\Omega}\|\boldsymbol{f}\|_{\infty,\Omega}\varepsilon^{-1}\right\}\,|||(\boldsymbol{v}_h, q_h)||| \\
&= \frac{\varepsilon^{-1/2}}{2}(1+\varepsilon^{-1/2})\,\gamma\,\|\boldsymbol{f}\|_{\infty,\Omega}\|p-p_h\|_{0,\Omega}\,|||(\boldsymbol{v}_h, q_h)||| \\
&\leq \frac{\varepsilon^{-1/2}}{2}(3+\varepsilon^{-1/2})\,\gamma\,\|\boldsymbol{f}\|_{\infty,\Omega}\|p-p_h\|_{0,\Omega}\,|||(\boldsymbol{v}_h, q_h)|||,
\end{aligned}$$

and the result follows. □

Theorem 6 (*Main Result*)**.** *Let $(\boldsymbol{u}, p) \in H^{k+1}(\Omega)^d \cap \boldsymbol{H} \times H^{k+1}(\Omega)$, be the solution of (2.5) and $(\boldsymbol{u}_h, p_h) \in \boldsymbol{H}_h \times Q_h$ solution of (3.1). If we assume (3.6), then it holds*

$$|||(\boldsymbol{u}-\boldsymbol{u}_h, p-p_h)||| \leq C\,h^k\left\{(\varepsilon^{1/2}+1)\,\|\boldsymbol{u}\|_{k+1,\Omega} + (\varepsilon^{-1/2}+\varepsilon^{-1}+1)\,\|p\|_{k+1,\Omega}\right\},$$

with $C > 0$ independent of h and ε.

Proof. Let

$$(\eta^{\boldsymbol{u}}, \eta^p) := (\boldsymbol{u} - \boldsymbol{I}_h\boldsymbol{u}, p - \mathcal{J}_h p) \quad \text{and} \quad (e_h^{\boldsymbol{u}}, e_h^p) := (\boldsymbol{u}_h - \boldsymbol{I}_h\boldsymbol{u}, p_h - \mathcal{J}_h p).$$

Using the definition of B_{stab} given in (3.2), and Cauchy–Schwarz inequality, we have

$$\begin{aligned}
&B_{\text{stab}}((\eta^{\boldsymbol{u}}, \eta^p), (\boldsymbol{v}_h, q_h)) \\
&= \varepsilon(\eta^{\boldsymbol{u}}, \boldsymbol{v}_h) + (\eta^p, \nabla\cdot\boldsymbol{v}_h) - (q_h, \nabla\cdot\eta^{\boldsymbol{u}}) - \frac{1}{2}\big(\varepsilon^{-1}(\varepsilon\eta^{\boldsymbol{u}} - \nabla\eta^p), \varepsilon\boldsymbol{v}_h + \nabla q_h\big) + \varepsilon\,(\nabla\cdot\eta^{\boldsymbol{u}}, \nabla\cdot\boldsymbol{v}_h)
\end{aligned}$$

$$\le \Big\{ \varepsilon^{1/2}\|\eta^{\boldsymbol{u}}\|_{0,\Omega} + \varepsilon^{-1/2}\|\eta^p\|_{0,\Omega} + \|\nabla\cdot\eta^{\boldsymbol{u}}\|_{0,\Omega} + \frac{1}{2}(\varepsilon^{1/2}+1)\big[\|\eta^{\boldsymbol{u}}\|_{0,\Omega} + \varepsilon^{-1}\,|\eta^p|_{1,\Omega}\big]$$
$$+\varepsilon^{1/2}\|\nabla\cdot\eta^{\boldsymbol{u}}\|_{0,\Omega}\Big\}\, |||(\boldsymbol{v}_h,q_h)|||$$
$$\le \Big\{\frac{1}{2}(3\varepsilon^{1/2}+1)\|\eta^{\boldsymbol{u}}\|_{0,\Omega} + (\varepsilon^{1/2}+1)\|\nabla\cdot\eta^{\boldsymbol{u}}\|_{0,\Omega} + \varepsilon^{-1/2}\|\eta^p\|_{0,\Omega} + \frac{1}{2}\varepsilon^{-1}(\varepsilon^{1/2}+1)\,|\eta^p|_{1,\Omega}\Big\}\, |||(\boldsymbol{v}_h,q_h)|||. \tag{3.14}$$

Using Lemmas 3 and 5, and inequality (3.14), we get that

$$\begin{aligned}B_{\mathrm{stab}}((e_h^{\boldsymbol{u}},e_h^p),(\boldsymbol{v}_h,q_h)) &= B_{\mathrm{stab}}((\eta^{\boldsymbol{u}},\eta^p),(\boldsymbol{v}_h,q_h)) - B_{\mathrm{stab}}((\boldsymbol{u}-\boldsymbol{u}_h,p-p_h),(\boldsymbol{v}_h,q_h))\\
&\le\Big[\frac{1}{2}(3\varepsilon^{1/2}+1)\|\eta^{\boldsymbol{u}}\|_{0,\Omega} + (\varepsilon^{1/2}+1)\|\nabla\cdot\eta^{\boldsymbol{u}}\|_{0,\Omega} + \varepsilon^{-1/2}\|\eta^p\|_{0,\Omega}+\\
&\quad\frac{1}{2}\varepsilon^{-1}(\varepsilon^{1/2}+1)\,|\eta^p|_{1,\Omega}\Big]|||(\boldsymbol{v}_h,q_h)|||+\\
&\quad\frac{\varepsilon^{-1/2}}{2}(3+\varepsilon^{-1/2})\,\gamma\,\|\boldsymbol{f}\|_{\infty,\Omega}\|p-p_h\|_{0,\Omega}\,|||(\boldsymbol{v}_h,q_h)|||.\end{aligned}$$

Now, using Lemma 3 and (3.6), we have

$$\begin{aligned}&\beta_s\,|||(e_h^{\boldsymbol{u}},e_h^p)|||\\
&\le\frac{1}{2}(3\varepsilon^{1/2}+1)\|\eta^{\boldsymbol{u}}\|_{0,\Omega} + (\varepsilon^{1/2}+1)\|\nabla\cdot\eta^{\boldsymbol{u}}\|_{0,\Omega} + \varepsilon^{-1/2}\|\eta^p\|_{0,\Omega}+\\
&\quad\frac{1}{2}\varepsilon^{-1}(\varepsilon^{1/2}+1)\,|\eta^p|_{1,\Omega} + \frac{\varepsilon^{-1/2}}{2}(3+\varepsilon^{-1/2})\,\gamma\,\|\boldsymbol{f}\|_{\infty,\Omega}\|p-p_h\|_{0,\Omega}\\
&\le\frac{1}{2}(3\varepsilon^{1/2}+1)\|\eta^{\boldsymbol{u}}\|_{0,\Omega} + (\varepsilon^{1/2}+1)\|\nabla\cdot\eta^{\boldsymbol{u}}\|_{0,\Omega} + \varepsilon^{-1/2}\|\eta^p\|_{0,\Omega}+\\
&\quad\frac{1}{2}\varepsilon^{-1}(\varepsilon^{1/2}+1)\,|\eta^p|_{1,\Omega} + \frac{\varepsilon^{-1/2}}{2}(3+\varepsilon^{-1/2})\,\gamma\,\|\boldsymbol{f}\|_{\infty,\Omega}|||(\boldsymbol{u}-\boldsymbol{u}_h,p-p_h)|||\\
&\le\frac{1}{2}(3\varepsilon^{1/2}+1)\|\eta^{\boldsymbol{u}}\|_{0,\Omega} + (\varepsilon^{1/2}+1)\|\nabla\cdot\eta^{\boldsymbol{u}}\|_{0,\Omega} + \varepsilon^{-1/2}\|\eta^p\|_{0,\Omega}+\\
&\quad\frac{1}{2}\varepsilon^{-1}(\varepsilon^{1/2}+1)\,|\eta^p|_{1,\Omega} + \frac{\beta_s}{2}\,|||(\boldsymbol{u}-\boldsymbol{u}_h,p-p_h)|||.\end{aligned} \tag{3.15}$$

Furthermore, using the triangle inequality and (3.15), we obtain

$$\begin{aligned}|||(\boldsymbol{u}-\boldsymbol{u}_h,p-p_h)||| &\le |||(\eta^{\boldsymbol{u}},\eta^p)||| + C\Big\{(\varepsilon^{1/2}+1)\,\|\eta^{\boldsymbol{u}}\|_{\boldsymbol{H}} + \varepsilon^{-1/2}\|\eta^p\|_{0,\Omega} + \varepsilon^{-1}(\varepsilon^{1/2}+1)\,|\eta^p|_{1,\Omega}\Big\}\\
&\quad+\frac{1}{2}\,|||(\boldsymbol{u}-\boldsymbol{u}_h,p-p_h)|||,\end{aligned}$$

thus

$$|||(\boldsymbol{u}-\boldsymbol{u}_h,p-p_h)||| \le C\Big\{|||(\eta^{\boldsymbol{u}},\eta^p)||| + (\varepsilon^{1/2}+1)\,\|\eta^{\boldsymbol{u}}\|_{\boldsymbol{H}} + \varepsilon^{-1/2}\|\eta^p\|_{0,\Omega} + \varepsilon^{-1}\,(\varepsilon^{1/2}+1)\,|\eta^p|_{1,\Omega}\Big\}.$$

Finally, using the properties of $\boldsymbol{I}_h$ and $\mathcal{J}_h$, we have

$$|||(\eta^{\boldsymbol{u}},\eta^p)||| \le C\,h^k\Big\{\varepsilon^{1/2}\,\|\boldsymbol{u}\|_{k+1,\Omega} + \|p\|_{k+1,\Omega}\Big\},$$

and the result follows. □

4. A posteriori error analysis

In this section, we present a residual a posteriori error estimator for the stabilized finite element method (3.1). Let $\Gamma_{D,h}$ be the partition of Γ_D inherited from the triangulation $\mathcal{T}_h$, and define the mesh size $h_D := \max\{|F| : F \in \Gamma_{D,h}\}$. For simplicity, we assume that

- $\boldsymbol{f}$ is a piecewise polynomial in Ω; i.e $\boldsymbol{f}\Big|_K \in \mathbb{P}_l(K)^d$, $\forall K \in \mathcal{T}_h$, $l \geq 0$.
- φ is a continuous piecewise polynomial in $\Gamma_{D,h}$, i.e $\varphi \in C^0(\Gamma_{D,h})$, $\varphi\Big|_F \in \mathbb{P}_l(F)$, $\forall F \in \Gamma_{D,h}$, $l \geq 0$.

Remark 4. If $\boldsymbol{f}$ is not a piecewise polynomial, then some oscillatory terms will appear in our a posteriori bounds in a standard way. We made this assumption only for a clarity matter.

For each $K \in \mathcal{T}_h$ and each $F \in \mathcal{E}_D$, we define the residuals

$$\boldsymbol{\mathcal{R}}_K := \Big(\gamma\,(p_h+1)\boldsymbol{f} - \varepsilon\,\boldsymbol{u}_h + \nabla p_h\Big)\Big|_K,$$
$$\mathcal{R}_F := (\varphi - p_h)\Big|_F.$$

Thus, our residual-based error estimator is given by

$$\eta := \left\{ \sum_{K\in\mathcal{T}_h} \eta_K^2 \right\}^{1/2}, \tag{4.1}$$

where, for each $K \in \mathcal{T}_h$, we have that

$$\eta_K^2 := \|\boldsymbol{\mathcal{R}}_K\|_{0,K}^2 + \varepsilon^2\,\|\nabla\cdot\boldsymbol{u}_h\|_{0,K}^2 + \sum_{F\subset\mathcal{E}(K)\cap\mathcal{E}_D} h_F^{-1}\,\|\mathcal{R}_F\|_{0,F}^2. \tag{4.2}$$

Lemma 7. *Let $(\boldsymbol{u}, p) \in \boldsymbol{H} \times Q$ and $(\boldsymbol{u}_h, p_h) \in \boldsymbol{H}_h \times Q_h$, be the solutions of (2.5) and (3.1), respectively. Then, for all $(\boldsymbol{v}, q) \in \boldsymbol{H} \times Q$, we have*

$$\begin{aligned}
&B_{\text{stab}}((\boldsymbol{u}-\boldsymbol{u}_h, p-p_h), (\boldsymbol{v}, q))\\
&= \langle \boldsymbol{v}\cdot\boldsymbol{n}, \varphi - p_h\rangle_{\Gamma_D} + \frac{1}{2}\left(\varepsilon^{-1/2}\gamma(p-p_h)\boldsymbol{f}, \varepsilon^{1/2}\boldsymbol{v} - \varepsilon^{-1/2}\nabla q\right)\\
&\quad + \frac{1}{2}\sum_{K\in\mathcal{T}_h}\left(\varepsilon^{-1/2}(\boldsymbol{\mathcal{R}}_K), \varepsilon^{1/2}\boldsymbol{v} - \varepsilon^{-1/2}\nabla q\right)_K + (q, \nabla\cdot\boldsymbol{u}_h) - \varepsilon\,(\nabla\cdot\boldsymbol{u}_h, \nabla\cdot\boldsymbol{v}).
\end{aligned}$$

Proof. Using (2.6), (2.7), (3.1) and integration by parts, we get that

$$\begin{aligned}
&B_{\text{stab}}((\boldsymbol{u}-\boldsymbol{u}_h, p-p_h), (\boldsymbol{v}, q))\\
=&B_{\text{stab}}((\boldsymbol{u}, p), (\boldsymbol{v}, q)) - B_{\text{stab}}((\boldsymbol{u}_h, p_h), (\boldsymbol{v}, q))\\
=&\langle \boldsymbol{v}\cdot\boldsymbol{n}, \varphi\rangle_{\Gamma_D} + \gamma((p+1)\boldsymbol{f}, \boldsymbol{v}) - \frac{1}{2}\left(\varepsilon^{-1}(\gamma\,(p+1)\boldsymbol{f}), \varepsilon\boldsymbol{v} + \nabla q\right)\\
&- \varepsilon\,(\boldsymbol{u}_h, \boldsymbol{v}) - (p_h, \nabla\cdot\boldsymbol{v}) + (q, \nabla\cdot\boldsymbol{u}_h) + \frac{1}{2}\left(\varepsilon^{-1}(\varepsilon\boldsymbol{u}_h - \nabla p_h), \varepsilon\boldsymbol{v} + \nabla q\right) - \varepsilon\,(\nabla\cdot\boldsymbol{u}_h, \nabla\cdot\boldsymbol{v})\\
=&\langle \boldsymbol{v}\cdot\boldsymbol{n}, \varphi\rangle_{\Gamma_D} + \gamma((p+1)\boldsymbol{f}, \boldsymbol{v}) + \varepsilon\,(\nabla\cdot\boldsymbol{u}, \nabla\cdot\boldsymbol{v}) - \varepsilon\,(\boldsymbol{u}_h, \boldsymbol{v}) - (p_h, \nabla\cdot\boldsymbol{v}) + (q, \nabla\cdot\boldsymbol{u}_h)\\
&+ \frac{1}{2}\left(\varepsilon^{-1}(\varepsilon\boldsymbol{u}_h - \nabla p_h - \gamma\,(p+1)\boldsymbol{f}), \varepsilon\boldsymbol{v} + \nabla q\right) - \varepsilon\,(\nabla\cdot\boldsymbol{u}_h, \nabla\cdot\boldsymbol{v})\\
=&\langle \boldsymbol{v}\cdot\boldsymbol{n}, \varphi - p_h\rangle_{\Gamma_D} + (\gamma(p+1)\boldsymbol{f} - \varepsilon\,\boldsymbol{u}_h + \nabla p_h, \boldsymbol{v}) + \varepsilon\,(\nabla\cdot\boldsymbol{u}, \nabla\cdot\boldsymbol{v}) + (q, \nabla\cdot\boldsymbol{u}_h)\\
&+ \frac{1}{2}\left(\varepsilon^{-1}(\varepsilon\boldsymbol{u}_h - \nabla p_h - \gamma\,(p+1)\boldsymbol{f}), \varepsilon\boldsymbol{v} + \nabla q\right) - \varepsilon\,(\nabla\cdot\boldsymbol{u}_h, \nabla\cdot\boldsymbol{v})\\
=&\langle \boldsymbol{v}\cdot\boldsymbol{n}, \varphi - p_h\rangle_{\Gamma_D} + (\gamma(p-p_h)\boldsymbol{f}, \boldsymbol{v}) + (\gamma(p_h+1)\boldsymbol{f} - \varepsilon\,\boldsymbol{u}_h + \nabla p_h, \boldsymbol{v}) + \varepsilon\,(\nabla\cdot\boldsymbol{u}, \nabla\cdot\boldsymbol{v}) + (q, \nabla\cdot\boldsymbol{u}_h)\\
&- \frac{1}{2}\left(\varepsilon^{-1}(\gamma\,(p-p_h)\boldsymbol{f}), \varepsilon\boldsymbol{v} + \nabla q\right) + \frac{1}{2}\left(\varepsilon^{-1}(\varepsilon\boldsymbol{u}_h - \nabla p_h - \gamma\,(p_h+1)\boldsymbol{f}), \varepsilon\boldsymbol{v} + \nabla q\right) - \varepsilon\,(\nabla\cdot\boldsymbol{u}_h, \nabla\cdot\boldsymbol{v})\\
=&\langle \boldsymbol{v}\cdot\boldsymbol{n}, \varphi - p_h\rangle_{\Gamma_D} + (\gamma(p-p_h)\boldsymbol{f}, \boldsymbol{v}) + \sum_{K\in\mathcal{T}_h}(\boldsymbol{\mathcal{R}}_K, \boldsymbol{v})_K + \varepsilon\,(\nabla\cdot\boldsymbol{u}, \nabla\cdot\boldsymbol{v}) + (q, \nabla\cdot\boldsymbol{u}_h)\\
&- \frac{1}{2}\left(\varepsilon^{-1}(\gamma\,(p-p_h)\boldsymbol{f}), \varepsilon\boldsymbol{v} + \nabla q\right) - \frac{1}{2}\sum_{K\in\mathcal{T}_h}\left(\varepsilon^{-1}(\boldsymbol{\mathcal{R}}_K), \varepsilon\boldsymbol{v} + \nabla q\right)_K - \varepsilon\,(\nabla\cdot\boldsymbol{u}_h, \nabla\cdot\boldsymbol{v})
\end{aligned}$$

$$
\begin{aligned}
=&\langle \boldsymbol{v}\cdot\boldsymbol{n}, \varphi - p_h\rangle_{\Gamma_D} + \frac{1}{2}(\varepsilon^{-1/2}\gamma(p-p_h)\boldsymbol{f}, \varepsilon^{1/2}\boldsymbol{v} - \varepsilon^{-1/2}\nabla q)\\
&+ \frac{1}{2}\sum_{K\in\mathcal{T}_h}\left(\varepsilon^{-1/2}(\boldsymbol{\mathcal{R}}_K), \varepsilon^{1/2}\boldsymbol{v} - \varepsilon^{-1/2}\nabla q\right)_K + (q, \nabla\cdot\boldsymbol{u}_h) - \varepsilon(\nabla\cdot\boldsymbol{u}_h, \nabla\cdot\boldsymbol{v}),
\end{aligned}
$$

and the result follows. □

To introduce the main result of this section, we need to define the following mesh-dependent norm for the pressure

$$
\|p\|_{\omega_F} := \left\{\sum_{K\in\omega_F}\left[h_K^{-2}\|p\|_{0,K}^2 + |p|_{1,K}^2\right]\right\}^{1/2},
$$

for all $p \in Q$, and for all $F \in \mathcal{E}_h$, where ω_F is the set of elements K of $\mathcal{T}_h$ such that $F \in \partial K$.

Lemma 8. *There exists $C > 0$, independent of h, such that*

$$
\|\psi\|_{0,\partial K}^2 \le C\left\{h_K^{-1}\|\psi\|_{0,K}^2 + h_K|\psi|_{1,K}^2\right\},
$$

for all $K \in \mathcal{T}_h$ and all $\psi \in H^1(K)$.

Proof. See [44, Theorem 3.10] or [45, (10.3.8)]. □

We are ready to prove the efficiency and reliability of the error estimator (4.1).

Theorem 9. *Let $(\boldsymbol{u}, p) \in \boldsymbol{H} \times Q$ and $(\boldsymbol{u}_h, p_h) \in \boldsymbol{H}_h \times Q_h$, be the solutions of* (2.5) and (3.1)*, respectively, and suppose valid* (3.6)*. Then, the following holds*

$$
|\!|\!|(\boldsymbol{u}-\boldsymbol{u}_h, p-p_h)|\!|\!| \le C\,\varepsilon^{-1/2}\max\left\{1, \varepsilon^{-1/2}\right\}\eta,
$$

where $C > 0$ is independent of ε, γ and h, and

$$
\eta_K^2 \le C\left\{\varepsilon^2\|\boldsymbol{u}-\boldsymbol{u}_h\|_{\mathrm{div},K}^2 + \beta_K^2\|p-p_h\|_{1,K}^2 + \sum_{F\subset\mathcal{E}(K)\cap\mathcal{E}_D}\|p-p_h\|_{\omega_F}^2\right\},
$$

for all $K \in \mathcal{T}_h$, where $\beta_K := \max\left\{\gamma\,\|\boldsymbol{f}\|_{\infty,\Omega}, 1\right\}$.

Proof. From [46,47] we have the following inverse estimate $\|\varphi - p_h\|_{1/2,\Gamma_D} \le C h_D^{-1/2}\|\varphi - p_h\|_{0,\Gamma_D}$, thus using Cauchy–Schwarz inequality, the definition of norm $\|\cdot\|_{-1/2,\Gamma_D}$ given in (2.10) and Lemma 7, we get

$$
\begin{aligned}
&B_{\mathrm{stab}}((\boldsymbol{u}-\boldsymbol{u}_h, p-p_h), (\boldsymbol{v}, q))\\
\le& C\,\|\boldsymbol{v}\cdot\boldsymbol{n}\|_{-1/2,\Gamma_D}\|\varphi - p_h\|_{1/2,\Gamma_D} + \frac{1}{2}\varepsilon^{-1/2}\|p-p_h\|_{0,\Omega}\,\gamma\,\|\boldsymbol{f}\|_{\infty,\Omega}\,\|\varepsilon^{1/2}\boldsymbol{v} - \varepsilon^{-1/2}\nabla q\|_{0,\Omega} +\\
&\frac{1}{2}\sum_{K\in\mathcal{T}_h}\varepsilon^{-1/2}\|\boldsymbol{\mathcal{R}}_K\|_{0,K}\|\varepsilon^{1/2}\boldsymbol{v} - \varepsilon^{-1/2}\nabla q\|_{0,K} + \|q\|_{0,\Omega}\|\nabla\cdot\boldsymbol{u}_h\|_{0,\Omega} + \varepsilon\,\|\nabla\cdot\boldsymbol{u}_h\|_{0,\Omega}\|\nabla\cdot\boldsymbol{v}\|_{0,\Omega}\\
\le& C\,h_D^{-1/2}\|\boldsymbol{v}\|_{\boldsymbol{H}}\|\varphi - p_h\|_{0,\Gamma_D} + \frac{1}{2}\varepsilon^{-1/2}\|p-p_h\|_{0,\Omega}\,\gamma\,\|\boldsymbol{f}\|_{\infty,\Omega}\,\|\varepsilon^{1/2}\boldsymbol{v} - \varepsilon^{-1/2}\nabla q\|_{0,\Omega} +\\
&\frac{1}{2}\sum_{K\in\mathcal{T}_h}\varepsilon^{-1/2}\|\boldsymbol{\mathcal{R}}_K\|_{0,K}\|\varepsilon^{1/2}\boldsymbol{v} - \varepsilon^{-1/2}\nabla q\|_{0,K} + \|q\|_{0,\Omega}\|\nabla\cdot\boldsymbol{u}_h\|_{0,\Omega} + \varepsilon\,\|\nabla\cdot\boldsymbol{u}_h\|_{0,\Omega}\|\nabla\cdot\boldsymbol{v}\|_{0,\Omega}\\
\le& C\,\|\boldsymbol{v}\|_{\boldsymbol{H}}\left\{\sum_{F\subset\mathcal{E}_D}h_F^{-1}\,\|\varphi - p_h\|_{0,F}^2\right\}^{1/2} + \frac{1}{2}\varepsilon^{-1/2}\|p-p_h\|_{0,\Omega}\,\gamma\,\|\boldsymbol{f}\|_{\infty,\Omega}\,\left\{\varepsilon^{1/2}\,\|\boldsymbol{v}\|_{0,\Omega} + \varepsilon^{-1/2}\,|q|_{1,\Omega}\right\} +\\
&C\left\{\sum_{K\in\mathcal{T}_h}\left[\varepsilon^{-1}\,\|\boldsymbol{\mathcal{R}}_K\|_{0,K}^2 + \varepsilon\,\|\nabla\cdot\boldsymbol{u}_h\|_{0,K}^2\right]\right\}^{1/2}
\end{aligned}
$$

$$
\begin{aligned}
&\times \left\{ \sum_{K\in\mathcal{T}_h} \left[\varepsilon \|\boldsymbol{v}\|_{0,K}^2 + \varepsilon\, \|\nabla\cdot\boldsymbol{v}\|_{0,K}^2 + \varepsilon^{-1}\, \|q\|_{0,K}^2 + \varepsilon^{-1}\, |q|_{1,K}^2\right] \right\}^{1/2} \\
\leq& \frac{1}{2}\,\varepsilon^{-1/2} \|p-p_h\|_{0,\Omega}\,\gamma\,\|\boldsymbol{f}\|_{\infty,\Omega}\, \left\{\varepsilon^{1/2}\, \|\boldsymbol{v}\|_{0,\Omega} + \varepsilon^{-1/2}\, |q|_{1,\Omega}\right\} + \\
&C \left\{ \sum_{K\in\mathcal{T}_h} \left[\varepsilon^{-1}\, \|\boldsymbol{\mathcal{R}}_K\|_{0,K}^2 + \varepsilon\, \|\nabla\cdot\boldsymbol{u}_h\|_{0,K}^2 + \sum_{F\subset\mathcal{E}(K)\cap\mathcal{E}_D} \varepsilon^{-1} h_F^{-1}\, \|\mathcal{R}_F\|_{0,F}^2 \right] \right\}^{1/2} \left\{\varepsilon\|\boldsymbol{v}\|_{\boldsymbol{H}}^2 + \varepsilon^{-1}\, \|q\|_{1,\Omega}^2\right\}^{1/2} \\
\leq& \varepsilon^{-1/2} \max\left\{1, \varepsilon^{-1/2}\right\} \left\{ \frac{1}{2}\, \|p-p_h\|_{0,\Omega}\,\gamma\,\|\boldsymbol{f}\|_{\infty,\Omega} + C\,\eta \right\} |||(\boldsymbol{v},q)|||. \qquad (4.3)
\end{aligned}
$$

Additionally, from Lemma 11, (3.6) and (4.3), we arrive at

$$
\begin{aligned}
\beta_c\, |||(\boldsymbol{u}-\boldsymbol{u}_h, p-p_h)||| \leq& \sup_{(\boldsymbol{v},q)\in\boldsymbol{H}\times Q} \frac{B_{\text{stab}}((\boldsymbol{u}-\boldsymbol{u}_h, p-p_h),(\boldsymbol{v},q))}{|||(\boldsymbol{v},q)|||} \\
\leq& \varepsilon^{-1/2} \max\left\{1, \varepsilon^{-1/2}\right\} \frac{1}{2}\, \|p-p_h\|_{0,\Omega}\,\gamma\,\|\boldsymbol{f}\|_{\infty,\Omega} + C\,\varepsilon^{-1/2} \max\left\{1, \varepsilon^{-1/2}\right\}\,\eta \\
\leq& \frac{3+\varepsilon^{-1/2}}{2} \varepsilon^{-1/2}\, \|p-p_h\|_{1,\Omega}\,\gamma\,\|\boldsymbol{f}\|_{\infty,\Omega} + C\,\varepsilon^{-1/2} \max\left\{1, \varepsilon^{-1/2}\right\}\,\eta \\
\leq& \frac{\beta_c}{2} \|p-p_h\|_{1,\Omega} + C\,\varepsilon^{-1/2} \max\left\{1, \varepsilon^{-1/2}\right\}\,\eta,
\end{aligned}
$$

and therefore,

$$
|||(\boldsymbol{u}-\boldsymbol{u}_h, p-p_h)||| \leq C\,\varepsilon^{-1/2} \max\left\{1, \varepsilon^{-1/2}\right\}\,\eta.
$$

On the other hand, using the definition of $\boldsymbol{\mathcal{R}}_K$ and (2.5), we deduce that

$$
\begin{aligned}
\|\boldsymbol{\mathcal{R}}_K\|_{0,K} &= \|\gamma\, p_h\boldsymbol{f} + \gamma\,\boldsymbol{f} - \varepsilon\,\boldsymbol{u}_h + \nabla p_h\|_{0,K} \\
&= \|\gamma\, p_h\boldsymbol{f} + \varepsilon\, u - \gamma\, p\boldsymbol{f} - \nabla p - \varepsilon\,\boldsymbol{u}_h + \nabla p_h\|_{0,K} \\
&= \|\gamma\,(p_h-p)\boldsymbol{f} + \varepsilon\,(\boldsymbol{u}-\boldsymbol{u}_h) + \nabla(p_h-p)\|_{0,K} \\
&\leq \|p-p_h\|_{0,K}\,\gamma\, \|\boldsymbol{f}\|_{\infty,K} + \varepsilon\, \|\boldsymbol{u}-\boldsymbol{u}_h\|_{0,K} + |p-p_h|_{1,K}. \qquad (4.4)
\end{aligned}
$$

In addition, as $\nabla\cdot\boldsymbol{u}=0$ in Ω, we have

$$
\|\nabla\cdot\boldsymbol{u}_h\|_{0,K} = \|\nabla\cdot(\boldsymbol{u}-\boldsymbol{u}_h)\|_{0,K}. \qquad (4.5)
$$

Similarly, as $p=\varphi$ on Γ_D, using the triangle inequality, Lemma 8 and the mesh regularity, we have that

$$
h_F^{-1}\|\mathcal{R}_F\|_{0,F}^2 = h_F^{-1}\|p-p_h\|_{0,F}^2 \leq C \sum_{K\in\omega_F} \left[h_K^{-2}\|p-p_h\|_{0,K}^2 + |p-p_h|_{1,K}^2\right]. \qquad (4.6)
$$

Finally, using the definition of η_K and (4.4)–(4.6), we get the result. □

5. Numerical results

In this section we present some numerical tests that illustrate the performance of our adapted stabilized finite element method given in (3.1). In particular, we confirm the results presented in Theorem 6 and the quality of the a posteriori error estimator (4.1) for the Darcy equation (2.5).

The stabilized finite element scheme was implemented using the open source finite element library FEniCS [48]. Recall that we use the notation $\mathbb{P}_k^d \times \mathbb{P}_k$ to mean that the velocity and the pressure are approximated using piecewise continuous polynomials of total degree at most k.

We will use the following notation for the error in velocity and pressure, respectively

$$
e_{\boldsymbol{u}} := \|\boldsymbol{u}-\boldsymbol{u}_h\|_{\boldsymbol{H}}, \qquad \text{and} \qquad e_p := \|p-p_h\|_{1,\Omega},
$$

while the convergence rates are denoted by

$$r_m(x) = \frac{\log(e_x^i/e_x^{i-1})}{\log(h^i/h^{i-1})}, \quad \text{with } x \in \{\boldsymbol{u}, p\},$$

where m is the polynomial degree, h^i, h^{i-1}, and, e_x^i, e_x^{i-1} represent two consecutive mesh sizes and two consecutive errors, respectively.

Finally, we define the effectivity index E as follows

$$E := \frac{\eta}{|||(\boldsymbol{u} - \boldsymbol{u}_h, p - p_h)|||}.$$

Our adaptive algorithm is given by

Algorithm 1 Adaptivity procedure

Require: $\theta \in (0, 1)$ and a coarse mesh $\mathcal{T}_h$.

1: Solve the stabilized discrete scheme (3.1) on the current mesh.
2: For each $K \in \mathcal{T}_h$, compute the local error indicator η_K given by (4.2).
3: Given $K \in \mathcal{T}_h$ such that $\eta_K \geq \theta \max_{K' \in \mathcal{T}_h} \eta_{K'}$, mark K and generate a new mesh $\mathcal{T}_h$ refining the marked elements.
4: If the stop criterion is not satisfied, go to step 1.

5.1. Analytic solution

In this example, we will test the approximation capability of the stabilized method in a non-convex domain with a nearly singular solution close to the origin of coordinates. We will also show that our error estimator adapts the meshes where it is expected and has a good effectivity index.

In this case our domain is $\Omega := \{(x, y) \in \mathbb{R}^2 : x^2 + y^2 \leq 1\} \setminus (0, 1)^2$, with $\Gamma_N := (0, 1) \times \{0\} \cup \{0\} \times (0, 1)$ and $\Gamma_D := \partial\Omega \setminus \Gamma_N$. The data $\boldsymbol{f}$ and φ are such that the exact solution is given by

$$\boldsymbol{u}(x, y) := [(x - c)^2 + (y - c)^2]^{-1/2}(c - y, x - c), \quad p(x, y) := \frac{1 - x^2 - y^2}{(x - c)^2 + (y - c)^2},$$

where $c = 0.025$. For the drag function (2.4), we take $\alpha_0 = 1.0$, while $\gamma = 1, 10^{-2}, 10^{-4}$.

Note that in this case $\boldsymbol{f}(x, y) = [h(x, y)]^{-1}\big(f_1(x, y), f_2(x, y)\big)$, where

$$f_1(x, y) = \frac{c - y}{\sqrt{(x - c)^2 + (y - c)^2}} + \frac{2x}{\varepsilon((x - c)^2 + (y - c)^2)} + \frac{(1 - x^2 - y^2)(2x - 2c)}{\varepsilon((x - c)^2 + (y - c)^2)^2}$$

$$f_2(x, y) = \frac{x - c}{\sqrt{(x - c)^2 + (y - c)^2}} + \frac{2y}{\varepsilon((x - c)^2 + (y - c)^2)} + \frac{(1 - x^2 - y^2)(2y - 2c)}{\varepsilon((x - c)^2 + (y - c)^2)^2}$$

$$h(x, y) = \frac{\left[1 - x^2 - y^2 + (c - x)^2 + (c - y)^2\right]}{\left[(c - x)^2 + (c - y)^2\right]}.$$

In this experiment, we consider a post-processed pressure $\tilde{p}_h := \frac{1}{\gamma}\log(p_h + 1)$ used to approximate the exact pressure $\tilde{p}$ of the original problem (2.1). In Tables 1–6 we show the approximation error using $\mathbb{P}_1^2 \times \mathbb{P}_1$ and $\mathbb{P}_2^2 \times \mathbb{P}_2$. We note that the errors on the velocity and pressure have the order predicted by Theorem 6. In particular, we have a better order for the velocity in the norm $\|\cdot\|_{\boldsymbol{H}}$ because the velocities considered are smooth functions. On the other hand, the error estimator η, given by (4.1), has a quite good quality reflected on the fact that effectivity indexes are close to the unity. Note that there is a small degradation of the effectivity index when ε goes to 0, because the contribution of the velocity norm $\|\boldsymbol{u} - \boldsymbol{u}_h\|_{\boldsymbol{H}}$ in the total error is negligible when $\varepsilon \to 0$, and by (4.4) and (4.6), the estimator η to be asymptotically smaller than $\|p - p_h\|_{1,\Omega}$ and therefore the effectivity index decreases. On the other hand, when the order of the interpolation polynomials is increased in our discrete scheme, now the velocity norm $\|\boldsymbol{u} - \boldsymbol{u}_h\|_{\boldsymbol{H}}$ in the total error is not negligible when $\varepsilon \to 0$ and therefore the effectivity index increased.

In Fig. 1 we show some of the adapted meshes obtained with Algorithm 1. Note that most of the refinement is close to the origin due to the fact that the exact solution has a singularity at the point (c, c) with $c = 0.025$, which

Table 1
$\mathbb{P}_1^2 \times \mathbb{P}_1$ stabilized scheme with a quasi-uniform refinement and $\varepsilon = 1$.

h	$\|\tilde{p} - \tilde{p}_h\|_{0,\Omega}$	$r_1(\tilde{p})$	$\|p - p_h\|_{1,\Omega}$	$r_1(p)$	$\|\boldsymbol{u} - \boldsymbol{u}_h\|_{\boldsymbol{H}}$	$r_1(u)$	$\|\|(\boldsymbol{u} - \boldsymbol{u}_h, p - p_h)\|\|$	η	E
0.079946	1.0710	–	2056.657064	–	54.729693	–	2111.386757	1888.309544	0.894346
0.039990	0.3093	1.8237	1318.996805	0.641253	28.518113	0.941022	1347.514919	1315.964898	0.976587
0.019998	0.0973	1.6963	868.049234	0.603722	13.842753	1.042973	881.891987	854.508058	0.968949
0.010000	0.0428	1.1913	463.443573	0.905514	5.588739	1.308725	469.032312	460.407948	0.981612
0.005000	0.0085	2.3461	235.075873	0.979267	1.851054	1.594176	236.926927	234.680437	0.990518
0.002500	0.0013	2.5169	115.909138	1.020132	0.579464	1.675556	116.488602	115.857322	0.994581

Table 2
$\mathbb{P}_1^2 \times \mathbb{P}_1$ stabilized scheme with a quasi-uniform refinement and $\varepsilon = 10^{-2}$.

h	$\|\tilde{p} - \tilde{p}_h\|_{0,\Omega}$	$r_1(\tilde{p})$	$\|p - p_h\|_{1,\Omega}$	$r_1(p)$	$\|\boldsymbol{u} - \boldsymbol{u}_h\|_{\boldsymbol{H}}$	$r_1(u)$	$\|\|(\boldsymbol{u} - \boldsymbol{u}_h, p - p_h)\|\|$	η	E
0.079946	105.3769	–	2055.714421	–	5464.968894	–	2602.211310	1884.365482	0.724140
0.039990	30.9629	1.7985	1319.171243	0.640401	2851.557217	0.939039	1604.326965	1316.475766	0.820578
0.020000	9.6558	1.7087	868.110785	0.603812	1381.329850	1.045919	1006.243770	854.723621	0.849420
0.010000	4.2576	1.1872	463.470837	0.905531	558.754010	1.305961	519.346238	460.505925	0.886703
0.005000	0.8452	2.3475	235.078411	0.979337	185.072224	1.594125	253.585634	234.689286	0.925483
0.002500	0,1480	2.5137	115.909236	1.020147	57.943499	1.675370	121.703586	115.857687	0.951966

Table 3
$\mathbb{P}_1^2 \times \mathbb{P}_1$ stabilized scheme with a quasi-uniform refinement and $\varepsilon = 10^{-4}$.

h	$\|\tilde{p} - \tilde{p}_h\|_{0,\Omega}$	$r_1(\tilde{p})$	$\|p - p_h\|_{1,\Omega}$	$r_1(p)$	$\|\boldsymbol{u} - \boldsymbol{u}_h\|_{\boldsymbol{H}}$	$r_1(u)$	$\|\|(\boldsymbol{u} - \boldsymbol{u}_h, p - p_h)\|\|$	η	E
0.079946	10541.657	–	2055.705163	–	546489.178588	–	7520.596949	1884.326586	0.250555
0.039990	3096,2833	1.7990	1319.173081	0.640392	285155.519779	0.939019	4170.728279	1316.481140	0.315648
0.019998	965.5397	1.7088	868.112101	0.603811	138413.649790	1.045919	2252.248599	854.727871	0.379500
0.010000	425.7359	1.1873	463.471114	0.905533	55875.284002	1.308893	1022.223954	460.506911	0.450495
0.005000	84.5191	2.2376	235.078437	0.979337	18507.189808	1.594124	420.150335	234.689375	0.558584
0.002500	14.8034	2.5137	115.909237	1.020147	5794.347388	1.675368	173.852711	115.857691	0.666413

Table 4
$\mathbb{P}_2^2 \times \mathbb{P}_2$ stabilized scheme with a quasi-uniform refinement and $\varepsilon = 1$.

h	$\|\tilde{p} - \tilde{p}_h\|_{0,\Omega}$	$r_1(\tilde{p})$	$\|p - p_h\|_{1,\Omega}$	$r_2(p)$	$\|\boldsymbol{u} - \boldsymbol{u}_h\|_{\boldsymbol{H}}$	$r_2(u)$	$\|\|(\boldsymbol{u} - \boldsymbol{u}_h, p - p_h)\|\|$	η	E
0.0799	0.0862	–	1107.895742	–	60.328929	–	1167.701879	967.730613	0.828748
0.0399	0.0306	1.5064	470.076480	1.237528	18.287520	1.761370	488.364000	457.382915	0.936561
0.0199	0.0014	4.4855	169.449270	1.4726600	3.462993	2.410449	172.912263	170.783398	0.987688
0.0099	0,00022	2.6861	51.791285	1.710069	0.686595	2.335218	52.477880	51.906513	0.989112
0.0049	4.4e−05	2.3251	13.031846	1.990669	0.080419	3.094040	13.112265	13.041533	0.994606
0.0024	2.0e−06	4.4575	3.230428	2.012244	0.009300	3.112197	3.239729	3.230962	0.997294

Table 5
$\mathbb{P}_2^2 \times \mathbb{P}_2$ stabilized scheme with a quasi-uniform refinement and $\varepsilon = 10^{-2}$.

h	$\|\tilde{p} - \tilde{p}_h\|_{0,\Omega}$	$r_1(\tilde{p})$	$\|p - p_h\|_{1,\Omega}$	$r_2(p)$	$\|\boldsymbol{u} - \boldsymbol{u}_h\|_{\boldsymbol{H}}$	$r_2(u)$	$\|\|(\boldsymbol{u} - \boldsymbol{u}_h, p - p_h)\|\|$	η	E
0.079946	8.5929	–	1107.408226	–	6033.736118	–	1710.781838	967.887247	0.565757
0.039990	3,0673	1.4993	470.062955	1.237020	1828.499303	1.723048	652.912885	457.301064	0.700401
0.019998	0,1410	4.4846	169.448973	1.472322	346.295943	2.401102	204.078568	170.782099	0.836845
0.010000	0,0219	2.6682	51.791298	1.710316	68.659412	2.334812	58.657239	51.906578	0.884913
0.005000	0,0044	2.3364	13.031845	1.990668	8.041910	3.093847	13.836036	13.041530	0.942577
0.002500	1.88e−4	4.5372	3.230428	2.012244	0.930030	3.112189	3.323431	3.230962	0.972176

is close to $(0, 0)$. Finally, in Fig. 2 we compare the approximated solution, obtained by our proposed scheme, and the exact solution. Note that the approximated solution has a good agreement with the exact one.

Table 6
$\mathbb{P}_2^2 \times \mathbb{P}_2$ stabilized scheme with a quasi-uniform refinement and $\varepsilon = 10^{-4}$.

h	$\|\tilde{p} - \tilde{p}_h\|_{0,\Omega}$	$r_1(\tilde{p})$	$\|p - p_h\|_{1,\Omega}$	$r_2(p)$	$\|\boldsymbol{u} - \boldsymbol{u}_h\|_{\boldsymbol{H}}$	$r_2(u)$	$\|\|(\boldsymbol{u} - \boldsymbol{u}_h, p - p_h)\|\|$	η	E
0.079946	859,2656	–	1107.408586	–	603374.475161	–	7141.153338	967.888845	0.135537
0.039990	306,7392	1.4992	470.062821	1.237021	182849.680322	1.723453	2298.559625	457.300247	0.198951
0.019998	14,0967	4.4846	169.448970	1.472321	34629.590957	2.401101	515.744880	170.782086	0.331137
0.010000	2,1925	2.6882	51.791298	1.710316	6865.941117	2.334813	120.450710	51.906579	0.430936
0.005000	0,4371	2.3364	13.031845	1.990668	804.191016	3.093847	21.073755	13.041530	0.618852
0.002500	0.0188	4.5360	3.230428	2.012244	93.003039	3.112188	4.160459	3.230962	0.776588

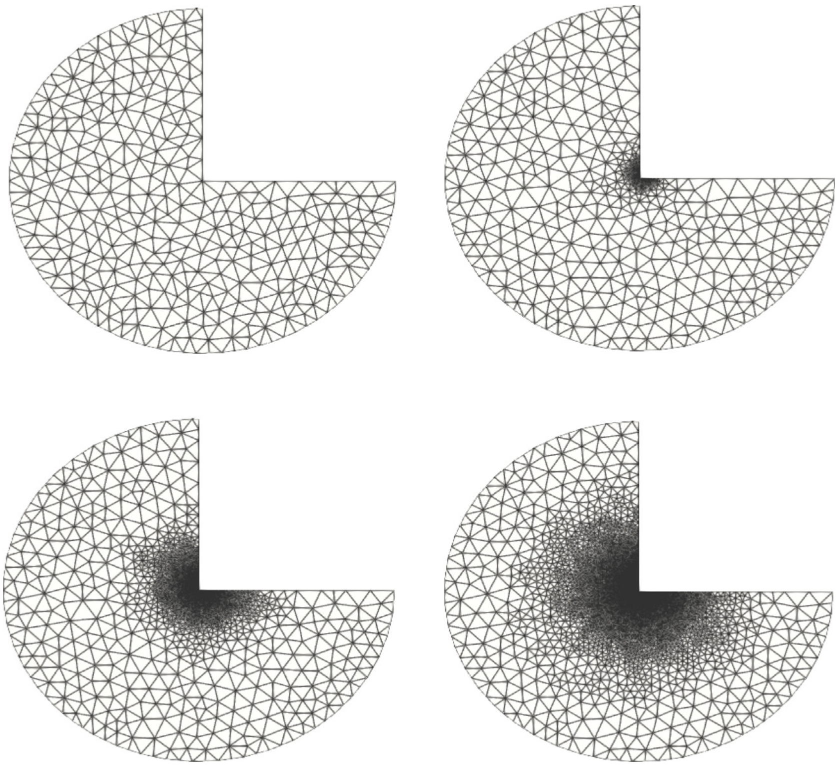

Fig. 1. Suite of adaptive meshes: $\mathcal{T}_{h,0}$ (top left), $\mathcal{T}_{h,8}$ (top right), $\mathcal{T}_{h,16}$ (bottom left) and $\mathcal{T}_{h,20}$ (bottom right).

5.2. A reservoir simulation

For our second problem, we have taken a reservoir problem from [16]. Here $\Omega := (0, 2) \times (0, 1)$, $\alpha_0 = 1$ and $\gamma = 0.005$. On Γ_D^1 we prescribe $p = p_{atm} = 1.0$ and on Γ_D^2, $p = p_{enh} = 5$. On the rest of the boundary we impose $\boldsymbol{v} \cdot \boldsymbol{n} = 0$ (see Fig. 3).

As in the previous example, we show in Fig. 4 some of the adapted meshes obtained with Algorithm 1. Note that most of the refinement is close to the Γ_D^1, which is consistent with the physics of the problem. Finally, in Figs. 5 and 6, we compare the approximated solution, obtained by our stabilized scheme, and the exact solution. Note that the approximated solution has a good agreement with the reference one.

5.3. A 3D simulation

Let $\Omega := (0, 1)^3$, and let $\boldsymbol{f}$ such that the exact solution is given by

$$\boldsymbol{u}(x, y, z) := \frac{1}{2}(-y^2, z^2, x^2) \qquad \text{and} \qquad p(x, y, z) := 2 + xyz.$$

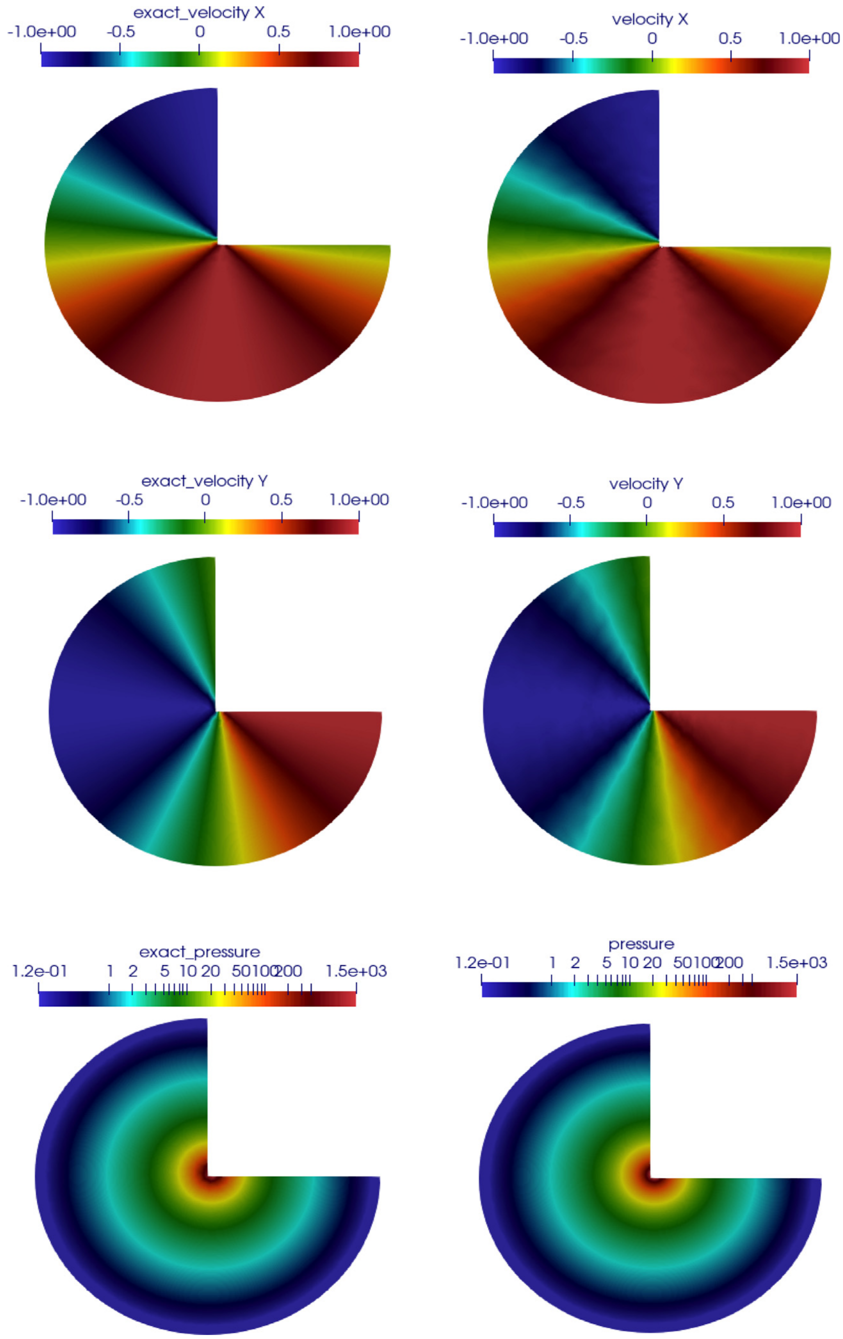

Fig. 2. Components of the exact solution (left column) compared with the approximated solution (right column) obtained using $\mathbb{P}_1^2 \times \mathbb{P}_1$ on the final adapted mesh of 178,596 elements.

We assume that $\Gamma_D := \{0\}\times]0,1[\times]0,1[\cup]0,1[\times\{0\}\times]0,1[\cup]0,1[\times]0,1[\times\{0\}$ with $\varphi := 2$, and $\Gamma_N := \partial\Omega \backslash \Gamma_D$. We choose $\alpha_0 = 1.0$ and $\gamma = 0.25$, i.e. $\varepsilon = 0.25$. Note that in this case we have $\boldsymbol{f}(x, y, z) := [h(x, y, z)]^{-1}\big(f_1(x, y, z), f_2(x, y, z), f_3(x, y, z)\big)$, where

$$f_1(x, y, z) = -\frac{1}{2}y^2 + \frac{1}{\varepsilon}yz$$

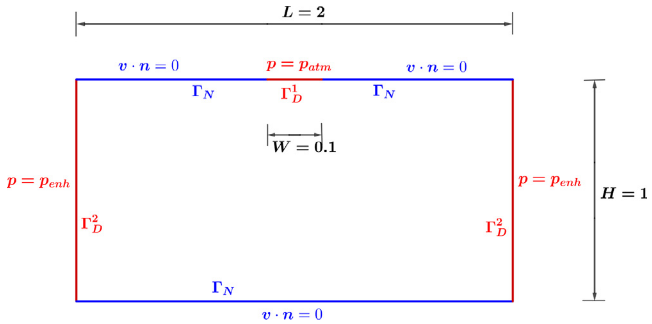

Fig. 3. Sketch of Ω with Dirichlet boundary conditions for the pressure in Γ_D^1 and Γ_D^2, and normal trace zero for the velocity in Γ_N.

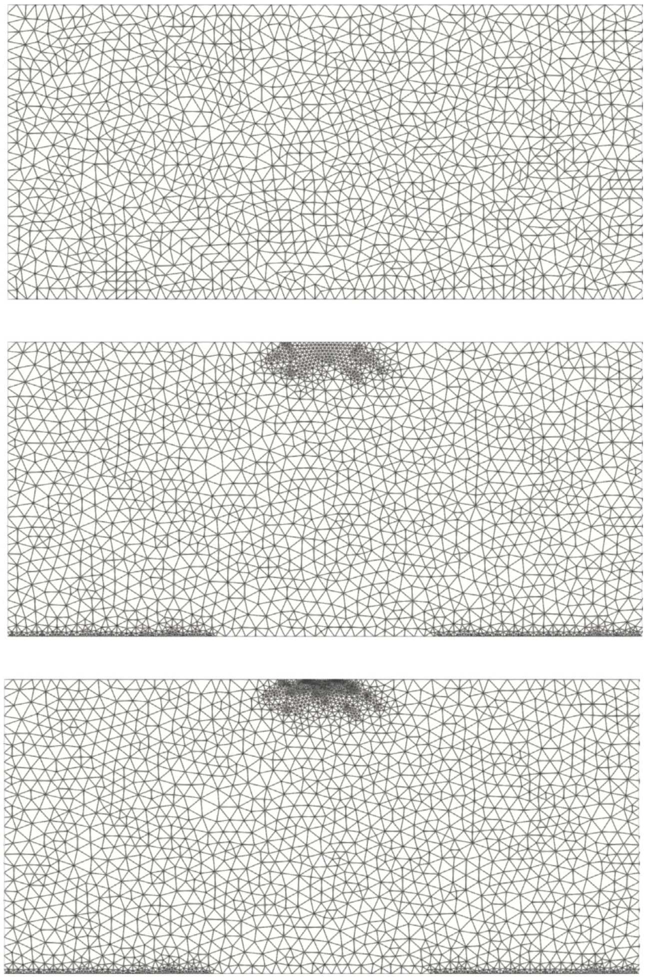

Fig. 4. Suite of adaptive meshes: $\mathcal{T}_{h,0}$ (top), $\mathcal{T}_{h,2}$ (middle) and $\mathcal{T}_{h,9}$ (bottom).

$$f_2(x, y, z) = \frac{1}{2}z^2 + \frac{1}{\varepsilon}xz$$
$$f_3(x, y, z) = \frac{1}{2}x^2 + \frac{1}{\varepsilon}xy$$
$$h(x, y, z) = 3 + xyz.$$

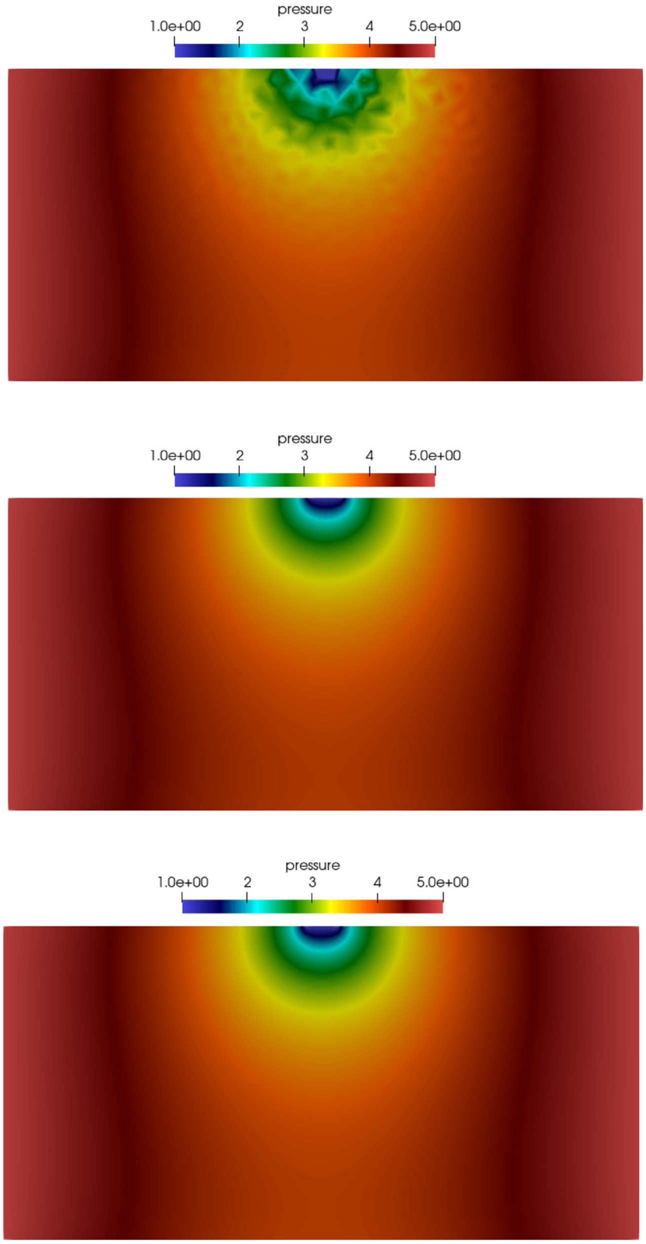

Fig. 5. Isolines of the pressure using $\mathbb{P}_1^2 \times \mathbb{P}_1$ finite element spaces, corresponding to the solution with 1,286 elements on the initial mesh (top), the solution with 6,994 elements on the adapted mesh (middle) and the reference solution on a fine uniform mesh with 773,034 elements (bottom).

In Table 7 we present the approximation errors and our a posteriori error estimator η. As in the two-dimensional case, we can see that the errors on the pressure $\|p - p_h\|_{0,\Omega}$ show a perfect agreement with those predicted by the theory, and on the velocity $\|\boldsymbol{u} - \boldsymbol{u}_h\|_{\boldsymbol{H}}$ again have a better order due to the smoothness of the solution. Moreover, the effectivity index for the residual a posteriori error estimator η is close to one.

Finally, we present the approximated solutions obtained with the stabilized scheme in a highly uniform refined mesh in Fig. 7. Here we used $\mathbb{P}_1^3 \times \mathbb{P}_1$ elements and we observe that the overall results are in accordance with the expected ones.

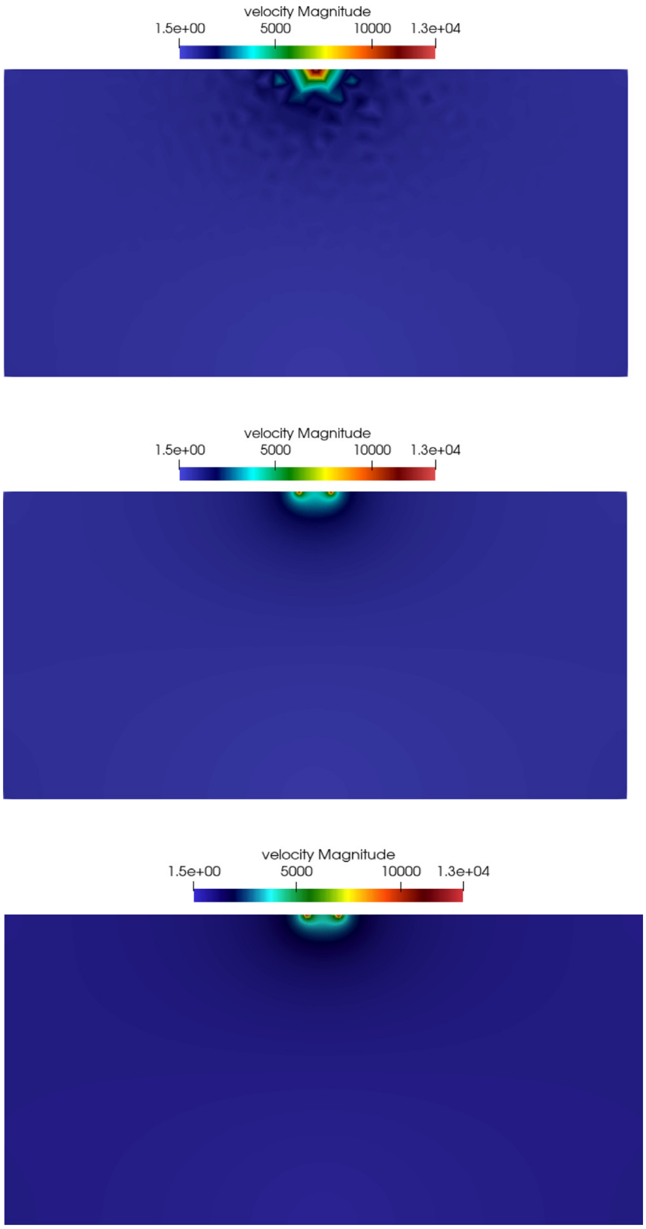

Fig. 6. Isolines of the velocity magnitude using $\mathbb{P}_1^2 \times \mathbb{P}_1$ finite element spaces, corresponding to the solution with 1,286 elements on the initial mesh (top), the solution with 6,994 elements on the adapted mesh (middle) and the reference solution on a fine uniform mesh with 773,034 elements (bottom).

6. Conclusions

In this work we introduced a new stabilized formulation for a Darcy equation, with an exponentially pressure-dependent porosity, in two or three dimensions. We included the well-posed results and a priori error analysis under standard assumptions. This new formulation enables us to use equal-order interpolation spaces for both velocity and pressure. Besides, we introduced and studied a residual-type a posteriori error estimator for this new stabilized formulation. In particular, we proved the equivalence between our error estimator and the approximation error. We also included numerical examples to demonstrate the theoretical results for both a priori and a posteriori error bounds. In the future, we will pursue the aim of extending this adaptive scheme to problems in which a fluid flow

Table 7
$\mathbb{P}_1^3 \times \mathbb{P}_1$ stabilized scheme with a quasi-uniform refinement and $\varepsilon = 0.25$.

h	$\|p - p_h\|_{1,\Omega}$	$r_1(p)$	$\|\boldsymbol{u} - \boldsymbol{u}_h\|_{\boldsymbol{H}}$	$r_1(u)$	$\|\|\|(\boldsymbol{u} - \boldsymbol{u}_h, p - p_h)\|\|\|$	η	E
0.866025	0.264920	–	0.232318	–	0.352355	0.279711	0.793833
0.433013	0.155252	0.770946	0.078652	1.562548	0.174038	0.162626	0.934427
0.216506	0.082301	0.915627	0.023047	1.770898	0.085467	0.086156	1.008067
0.108253	0.041952	0.972170	0.006394	1.849788	0.042436	0.043960	1.035904
0.054127	0.021103	0.991305	0.001730	1.885972	0.021173	0.022123	1.044853
0.027063	0.010570	0.997446	0.000462	1.904757	0.010580	0.011078	1.047037

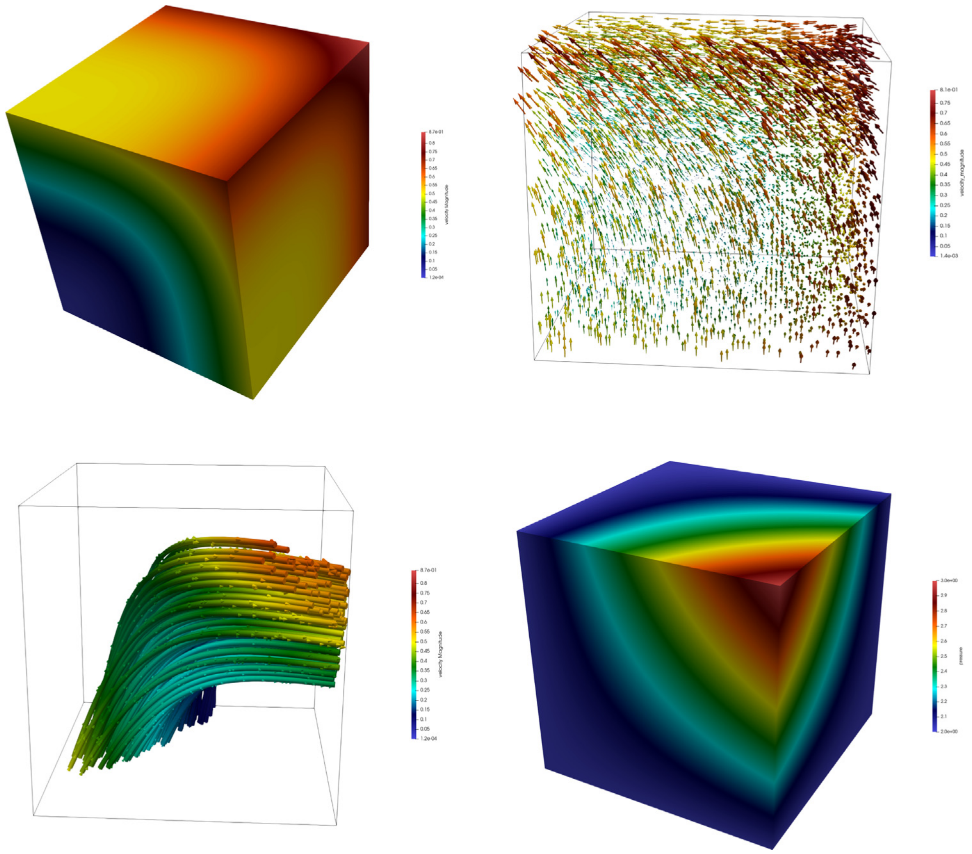

Fig. 7. Approximated solution. Velocity magnitude (top left), velocity vectors (top right), velocity streamlines (bottom left) and isovalues of the pressure (bottom right). We use $\mathbb{P}_1^3 \times \mathbb{P}_1$ elements on a uniform mesh of 1,572,864 elements.

(modeled by the Stokes or Navier–Stokes equation) is coupled with a porous media flow (modeled by the Darcy equation), which is a highly interesting problem for practitioners.

Declaration of competing interest

The authors declare that they have no known competing financial interests or personal relationships that could have appeared to influence the work reported in this paper.

Acknowledgments

The first author was partially supported by ANID-Chile through the project Centro de Modelamiento Matemático (AFB170001) of the PIA Program: Concurso Apoyo a Centros Científicos y Tecnológicos de Excelencia con

Financiamiento Basal, and Universidad de Concepción through project VRID 219.013.046-INV. The second author was partially supported by CONICYT-Chile through scholarship PCHA/Doctorado Nacional. The third author was partially supported by Dirección de Investigación e Innovación of the Universidad Católica de la Santísima Concepción through project DIREG 01/2020.

Appendix A

As it is well known, the bilinear form $b(\cdot,\cdot)$ does not satisfy an inf–sup condition, using the subspaces $\boldsymbol{H}_h$ and Q_h, but it satisfies the following weak inf–sup condition.

Lemma 10. *There exist positive constants β_w and λ, independent of ε and h, such that*

$$\sup_{\boldsymbol{v}_h\in\boldsymbol{H}_h}\frac{b(\boldsymbol{v}_h,p_h)}{\|\boldsymbol{v}_h\|_{\boldsymbol{H}}}\geq\beta_w\,\|p_h\|_{0,\Omega}-\lambda\,|p_h|_{1,\Omega}\qquad\forall p_h\in Q_h. \tag{A.1}$$

Proof. The proof of this result uses similar arguments to those used in [40, Lemma 3.3]. Let $p_h\in Q_h$, then there exist $\bar{p}_h\in\mathbb{R}$ and $p_h^*\in L_0^2(\Omega)$, such that $p_h=\bar{p}_h+p_h^*$. Additionally, there exists $\boldsymbol{w}\in H_0^1(\Omega)^d$ (see [12]) such that

$$(\nabla\cdot\boldsymbol{w},p_h)=(\nabla\cdot\boldsymbol{w},p_h^*)\geq C_1\|p_h^*\|_{0,\Omega}\|\boldsymbol{w}\|_{1,\Omega}. \tag{A.2}$$

Furthermore, let $\mathcal{C}_h\boldsymbol{w}\in\boldsymbol{H}_h\cap H_0^1(\Omega)^d$ the Clément interpolate of $\boldsymbol{w}$ (see [49]). This interpolation operator satisfies

$$\left\{\sum_{K\in\mathcal{T}_h}h_K^{-2}\|\boldsymbol{w}-\mathcal{C}_h\boldsymbol{w}\|_{0,K}^2\right\}^{1/2}\leq C_2\|\boldsymbol{w}\|_{1,\Omega}, \tag{A.3}$$

and

$$\|\mathcal{C}_h\boldsymbol{w}\|_{1,\Omega}\leq C_3\|\boldsymbol{w}\|_{1,\Omega}. \tag{A.4}$$

Using (A.2) and integration by parts, we get that

$$\begin{aligned}(\nabla\cdot\mathcal{C}_h\boldsymbol{w},p_h)&=(\nabla\cdot\mathcal{C}_h\boldsymbol{w},p_h^*)\\&=(\nabla\cdot(\mathcal{C}_h\boldsymbol{w}-\boldsymbol{w}),p_h^*)+(\nabla\cdot\boldsymbol{w},p_h^*)\\&\geq\sum_{K\in\mathcal{T}_h}(\mathcal{C}_h\boldsymbol{w}-\boldsymbol{w},\nabla p_h^*)_K+C_1\|p_h^*\|_{0,\Omega}\|\boldsymbol{w}\|_{1,\Omega}.\end{aligned}$$

Using Cauchy–Schwarz inequality and (A.3), we obtain

$$\begin{aligned}(\nabla\cdot\mathcal{C}_h\boldsymbol{w},p_h)&\geq-\left(\sum_{K\in\mathcal{T}_h}h_K^{-2}\|\mathcal{C}_h\boldsymbol{w}-\boldsymbol{w}\|_{0,K}^2\right)^{1/2}\left(\sum_{K\in\mathcal{T}_h}h_K^2\|\nabla p_h^*\|_{0,K}^2\right)^{1/2}+C_1\|p_h^*\|_{0,\Omega}\|\boldsymbol{w}\|_{1,\Omega}\\&\geq\left\{-C_2\left(\sum_{K\in\mathcal{T}_h}h_K^2\|\nabla p_h^*\|_{0,K}^2\right)^{1/2}+C_1\|p_h^*\|_{0,\Omega}\right\}\|\boldsymbol{w}\|_{1,\Omega},\end{aligned}$$

and, in consequence

$$\frac{(\nabla\cdot\mathcal{C}_h\boldsymbol{w},p_h)}{\|\boldsymbol{w}\|_{1,\Omega}}\geq C_1\|p_h^*\|_{0,\Omega}-C_2\left(\sum_{K\in\mathcal{T}_h}h_K^2\|\nabla p_h^*\|_{0,K}^2\right)^{1/2}. \tag{A.5}$$

We can assume (see [40]) that, for a reasonable mesh, there exist $\boldsymbol{z}_h\in\boldsymbol{H}_h$, $\boldsymbol{z}_h\neq\boldsymbol{0}$, such that

$$\frac{(\nabla\cdot\boldsymbol{z}_h,\bar{p}_h)}{\|\boldsymbol{z}_h\|_{1,\Omega}}\geq C_4\|\bar{p}_h\|_{0,\Omega}. \tag{A.6}$$

Let $\tilde{\boldsymbol{v}}_h := \|\boldsymbol{w}\|_{1,\Omega}^{-1}\mathcal{C}_h\boldsymbol{w} + \delta\|\boldsymbol{z}_h\|_{1,\Omega}^{-1}\boldsymbol{z}_h$, with $\delta > 0$. It is clear that $\tilde{\boldsymbol{v}}_h \in \boldsymbol{H}_h$ and using (A.5), (A.6), we get

$$
\begin{aligned}
(\nabla\cdot\tilde{\boldsymbol{v}}_h, p_h) &= \frac{(\nabla\cdot\mathcal{C}_h\boldsymbol{w}, p_h)}{\|\boldsymbol{w}\|_{1,\Omega}} + \delta\frac{(\nabla\cdot\boldsymbol{z}_h, \bar{p}_h)}{\|\boldsymbol{z}_h\|_{1,\Omega}} + \delta\,\frac{(\nabla\cdot\boldsymbol{z}_h, p_h^*)}{\|\boldsymbol{z}_h\|_{1,\Omega}} \\
&\geq C_1\|p_h^*\|_{0,\Omega} - C_2\left(\sum_{K\in\mathcal{T}_h} h_K^2\|\nabla p_h^*\|_{0,K}^2\right)^{1/2} + \delta C_4\|\bar{p}_h\|_{0,\Omega} - \delta C_5\|p_h^*\|_{0,\Omega} \\
&\geq C_6\|p_h\|_{0,\Omega} - C_7\left(\sum_{K\in\mathcal{T}_h} h_K^2\|\nabla p_h^*\|_{0,K}^2\right)^{1/2},
\end{aligned}
$$

assuming that $\delta < C_1/C_5$. On the other hand, note that the definition of $\tilde{\boldsymbol{v}}_h$ and (A.4) shows $\|\tilde{\boldsymbol{v}}_h\|_{\boldsymbol{H}} \leq C\|\tilde{\boldsymbol{v}}_h\|_{1,\Omega} \leq C\,C_3 + C\,\delta$, and hence, we have that

$$
\sup_{\boldsymbol{v}_h\in\boldsymbol{H}_h}\frac{(\nabla\cdot\boldsymbol{v}_h, p_h)}{\|\boldsymbol{v}_h\|_{\boldsymbol{H}}} \geq C_8\|p_h\|_{0,\Omega} - C_9\left(\sum_{K\in\mathcal{T}_h} h_K^2\|\nabla p_h\|_{0,K}^2\right)^{1/2},
$$

which conclude the proof. □

Lemma 11. *There exists a positive constant β_c, independent of ε, such that*

$$
\sup_{(\boldsymbol{v},q)\in\boldsymbol{H}\times Q}\frac{B_{\text{stab}}((\boldsymbol{u},p),(\boldsymbol{v},q))}{|||(\boldsymbol{v},q)|||} \geq \beta_c\,|||(\boldsymbol{v},q)|||, \tag{A.7}
$$

for all $(\boldsymbol{u},p)\in\boldsymbol{H}\times Q$.

Proof. Given $p\in L^2(\Omega)$, from [42], there exists $\boldsymbol{w}\in\boldsymbol{H}$ such that $\nabla\cdot\boldsymbol{w} = -p$ and $\|\boldsymbol{w}\|_{\boldsymbol{H}} \leq C\|p\|_{0,\Omega}$. Then, for $(\boldsymbol{v},q) := (\boldsymbol{u}-\delta\boldsymbol{w}, p)$, with $\delta > 0$, we have

$$
\begin{aligned}
B_{\text{stab}}((\boldsymbol{u},p),(\boldsymbol{v},q)) &= B_{\text{stab}}((\boldsymbol{u},p),(\boldsymbol{u},p)) - \delta\,B_{\text{stab}}((\boldsymbol{u},p),(\boldsymbol{w},0)) \\
&= B_{\text{stab}}((\boldsymbol{u},p),(\boldsymbol{u},p)) - \delta\left[B_{\text{stab}}((\boldsymbol{u},0),(\boldsymbol{w},0)) + B_{\text{stab}}((\boldsymbol{0},p),(\boldsymbol{w},0))\right] \\
&= \frac{1}{2}\varepsilon\,\|\boldsymbol{u}\|_{0,\Omega}^2 + \varepsilon\,\|\nabla\cdot\boldsymbol{u}\|_{0,\Omega}^2 + \frac{1}{2}\varepsilon^{-1}\,|p|_{1,\Omega}^2 \\
&\quad - \delta\left[\frac{1}{2}\varepsilon\,(\boldsymbol{u},\boldsymbol{w}) + \varepsilon\,(\nabla\cdot\boldsymbol{u},\nabla\cdot\boldsymbol{w}) + (p,\nabla\cdot\boldsymbol{w}) + \frac{1}{2}\,(\nabla p,\boldsymbol{w})\right] \\
&= \frac{1}{2}\varepsilon\,\|\boldsymbol{u}\|_{0,\Omega}^2 + \varepsilon\,\|\nabla\cdot\boldsymbol{u}\|_{0,\Omega}^2 + \frac{1}{2}\varepsilon^{-1}\,|p|_{1,\Omega}^2 \\
&\quad - \frac{\delta}{2}\varepsilon\,(\boldsymbol{u},\boldsymbol{w}) - \delta\varepsilon\,(\nabla\cdot\boldsymbol{u},\nabla\cdot\boldsymbol{w}) - \delta\,(p,\nabla\cdot\boldsymbol{w}) - \frac{\delta}{2}\,(\nabla p,\boldsymbol{w}) \\
&= \frac{1}{2}\varepsilon\,\|\boldsymbol{u}\|_{0,\Omega}^2 + \varepsilon\,\|\nabla\cdot\boldsymbol{u}\|_{0,\Omega}^2 + \frac{1}{2}\varepsilon^{-1}\,|p|_{1,\Omega}^2 + \delta\,\|p\|_{0,\Omega}^2 \\
&\quad - \frac{\delta}{2}\varepsilon\,(\boldsymbol{u},\boldsymbol{w}) - \delta\varepsilon\,(\nabla\cdot\boldsymbol{u},\nabla\cdot\boldsymbol{w}) - \frac{\delta}{2}\,(\nabla p,\boldsymbol{w}) \\
&\geq \frac{1}{2}\varepsilon\,\|\boldsymbol{u}\|_{0,\Omega}^2 + \varepsilon\,\|\nabla\cdot\boldsymbol{u}\|_{0,\Omega}^2 + \frac{1}{2}\varepsilon^{-1}\,|p|_{1,\Omega}^2 + \delta\,\|p\|_{0,\Omega}^2 \\
&\quad - \frac{\delta}{2}\varepsilon\,\|\boldsymbol{u}\|_{0,\Omega}\|\boldsymbol{w}\|_{0,\Omega} - \delta\varepsilon\,\|\nabla\cdot\boldsymbol{u}\|_{0,\Omega}\|\nabla\cdot\boldsymbol{w}\|_{0,\Omega} - \frac{\delta}{2}|p|_{1,\Omega}\|\boldsymbol{w}\|_{0,\Omega}.
\end{aligned}
$$

The result follows using similar arguments as in the proof of Lemma 3. □

References

[1] H. Darcy, Les Fontaines Publiques de la Ville de Dijon, Victor Dalmont, Paris, 1856.

[2] P.W. Bridgman, The physics of high pressure, Nature 131 (1933) 259, http://dx.doi.org/10.1038/131259a0.

[3] K.R. Rajagopal, On a hierarchy of approximate models for flows of incompressible fluids through porous solids, Math. Models Methods Appl. Sci. 17 (2) (2007) 215–252, http://dx.doi.org/10.1142/S0218202507001899.
[4] P.A. Raviart, J.M. Thomas, A mixed finite element method for 2-nd order elliptic problems, in: I. Galligani, E. Magenes (Eds.), Mathematical Aspects of Finite Element Methods, Springer–Verlag, Berlin, Heidelberg, 1977, pp. 292–315, http://dx.doi.org/10.1007/BFb0064470.
[5] F. Brezzi, J. Douglas, L. Marini, Two families of mixed finite elements for second order elliptic problems, Numer. Math. 47 (2) (1985) 217–235, http://dx.doi.org/10.1007/BF01389710.
[6] J.M. Urquiza, D. N'Dri, A. Garon, M.C. Delfour, A numerical study of primal mixed finite element approximations of Darcy equations, Commun. Numer. Methods. Eng. 22 (8) (2006) 901–915, http://dx.doi.org/10.1002/cnm.859.
[7] P. Bochev, C. Dohrmann, A computational study of stabilized, low-order C^0 finite element approximations of Darcy equations, Comput. Mech. 38 (4–5) (2006) 310–333, http://dx.doi.org/10.1007/s00466-006-0036-y.
[8] F. Brezzi, M. Fortin, L.D. Marini, Error analysis of piecewise constant pressure approximations of Darcy's law, Comput. Methods Appl. Mech. Engrg. 195 (13–16) (2006) 1547–1559, http://dx.doi.org/10.1016/j.cma.2005.05.027.
[9] T. Barrios, J. Cascón, M. González, A posteriori error analysis of an augmented mixed finite element method for Darcy flow, Comput. Methods Appl. Mech. Engrg. 283 (2015) 909–922, http://dx.doi.org/10.1016/j.cma.2014.10.035.
[10] Z. Lotfian, M.V. Sivaselvan, Mixed finite element formulation for dynamics of porous media, Internat. J. Numer. Methods Engrg. 115 (2) (2018) 141–171, http://dx.doi.org/10.1002/nme.5799.
[11] F. Morales, A conforming primal-dual mixed formulation for the 2D multiscale porous media flow problem, Comput. Appl. Math. 38 (2) (2019) http://dx.doi.org/10.1007/s40314-019-0808-6.
[12] V. Girault, P. Raviart, Finite Element Methods for Navier–Stokes Equations: Theory and Algorithms, Springer Series in Computational Mathematics, Springer-Verlag Berlin Heidelberg, 1986, http://dx.doi.org/10.1007/978-3-642-61623-5.
[13] L. Tobiska, R. Verfürth, Analysis of a streamline diffusion finite element method for the Stokes and Navier-Stokes equations, SIAM J. Numer. Anal. 33 (1) (1996) 107–127, http://dx.doi.org/10.1137/0733007, 1377246.
[14] L. Franca, S. Frey, T.R. Hughes, Stabilized finite element methods. I. Application to the advective-diffusive model, Comput. Methods Appl. Mech. Engrg. 95 (2) (1992) 253–276, http://dx.doi.org/10.1016/0045-7825(92)90143-8.
[15] A. Masud, J. Kwack, A stabilized mixed finite element method for the first-order form of advection–diffusion equation, Internat. J. Numer. Methods Fluids 57 (9) (2008) 1321–1348, http://dx.doi.org/10.1002/fld.1842.
[16] K.B. Nakshatrala, K. Rajagopal, A numerical study of fluids with pressure-dependent viscosity flowing through a rigid porous medium, Internat. J. Numer. Methods Fluids 67 (3) (2011) 342–368, http://dx.doi.org/10.1002/fld.2358.
[17] G. Barrenechea, F. Valentin, Consistent local projection stabilized finite element methods, SIAM J. Numer. Anal. 48 (5) (2010) 1801–1825, http://dx.doi.org/10.1137/090753334.
[18] L. Franca, C. Harder, F. Valentin, On a residual local projection method for the Darcy equation, C. R. Math. Acad. Sci. Paris 347 (17–18) (2009) 1105–1110, http://dx.doi.org/10.1016/j.crma.2009.06.016.
[19] R. Araya, G. Barrenechea, A. Poza, F. Valentin, Convergence analysis of a residual local projection finite element method for the Navier-Stokes equations, SIAM J. Numer. Anal. 50 (2) (2012) 669–699, http://dx.doi.org/10.1137/110829283.
[20] R. Codina, Analysis of a stabilized finite element approximation of the Oseen equations using orthogonal subscales, Appl. Numer. Math. 58 (3) (2008) 264–283, http://dx.doi.org/10.1016/j.apnum.2006.11.011.
[21] E. Burman, M.A. Fernández, P. Hansbo, Continuous interior penalty finite element method for Oseen's equations, SIAM J. Numer. Anal. 44 (3) (2006) 1248–1274, http://dx.doi.org/10.1137/040617686.
[22] R. Becker, M. Braack, A finite element pressure gradient stabilization for the Stokes equations based on local projections, Calcolo 38 (4) (2001) 173–199, http://dx.doi.org/10.1007/s10092-001-8180-4.
[23] G. Barrenechea, F. Valentin, Beyond pressure stabilization: a low-order local projection method for the Oseen equation, Internat. J. Numer. Methods Engrg. 86 (7) (2011) 801–815, http://dx.doi.org/10.1002/nme.3075.
[24] R. Araya, A. Poza, F. Valentin, A low-order local projection method for the incompressible Navier-Stokes equations in two- and three-dimensions, IMA J. Numer. Anal. 36 (1) (2016) 267–295, http://dx.doi.org/10.1093/imanum/drv004.
[25] A. Masud, T.J.R. Hughes, A stabilized mixed finite element method for Darcy flow, Comput. Methods Appl. Mech. Engrg. 191 (39–40) (2002) 4341–4370, http://dx.doi.org/10.1016/S0045-7825(02)00371-7.
[26] P. Hansbo, M. Larson, A. Massing, A stabilized cut finite element method for the Darcy problem on surfaces, Comput. Methods Appl. Mech. Engrg. 326 (2017) 298–318, http://dx.doi.org/10.1016/j.cma.2017.08.007.
[27] G. Barrenechea, L. Franca, F. Valentin, A Petrov-Galerkin enriched method: a mass conservative finite element method for the Darcy equation, Comput. Methods Appl. Mech. Engrg. 196 (21–24) (2007) 2449–2464, http://dx.doi.org/10.1016/j.cma.2007.01.004.
[28] E. Burman, P. Hansbo, A unified stabilized method for Stokes' and Darcy's equations, J. Comput. Appl. Math. 198 (1) (2007) 35–51, http://dx.doi.org/10.1016/j.cam.2005.11.022.
[29] M.R. Correa, A.F.D. Loula, Unconditionally stable mixed finite element methods for Darcy flow, Comput. Methods Appl. Mech. Engrg. 197 (17–18) (2008) 1525–1540, http://dx.doi.org/10.1016/j.cma.2007.11.025.
[30] M.R. Correa, J.C. Rodriguez, A.M. Farias, D. de Siqueira, P. Devloo, Hierarchical high order finite element spaces in $H(\mathrm{div},\Omega)\times H^1(\Omega)$ for a stabilized mixed formulation of Darcy problem, Comput. Math. Appl. 80 (5) (2020) 1117–1141, http://dx.doi.org/10.1016/j.camwa.2020.06.003.
[31] C. Harder, D. Paredes, F. Valentin, A family of multiscaled-mixed finite element methods for the Darcy equation with rough coefficients, J. Comput. Phys. 245 (2013) 107–130, http://dx.doi.org/10.1016/j.jcp.2013.03.019.
[32] O. Durán, P.R.B. Devloo, S.M. Gomes, F. Valentin, A multiscale hybrid method for Darcy's problems using mixed finite element local solvers, Comput. Methods Appl. Mech. Engrg. 354 (2019) 213–244, http://dx.doi.org/10.1016/j.cma.2019.05.013.

[33] M. Azaïez, F. Ben Belgacem, C. Bernardi, N. Chorfi, Spectral discretization of Darcy's equations with pressure dependent porosity, Appl. Math. Comput. 217 (5) (2010) 1838–1856, http://dx.doi.org/10.1016/j.amc.2010.06.014.
[34] E. Ahusborde, M. Azaïez, F. Ben Belgacem, C. Bernardi, Automatic simplification of Darcy's equations with pressure dependent permeability, ESAIM Math. Model. Numer. Anal. 47 (6) (2013) 1797–1820, http://dx.doi.org/10.1051/m2an/2013089.
[35] C. Bernardi, S. Maarouf, D. Yakoubi, Spectral discretization of an unsteady flow through a porous solid, Calcolo 53 (4) (2016) 659–690, http://dx.doi.org/10.1007/s10092-015-0168-6.
[36] V. Girault, F. Murat, A. Salgado, Finite element discretization of Darcy's equations with pressure dependent porosity, M2AN Math. Model. Numer. Anal. 44 (6) (2010) 1155–1191, http://dx.doi.org/10.1051/m2an/2010019.
[37] G. Gatica, R. Ruiz-Baier, G. Tierra, A mixed finite element method for Darcy's equations with pressure dependent porosity, Math. Comp. 85 (2016) 1–33, http://dx.doi.org/10.1090/mcom/2980.
[38] N. Mapakshi, J. Chang, K. Nakshatrala, A scalable variational inequality approach for flow through porous media models with pressure-dependent viscosity, J. Comput. Phys. 359 (2018) 137–163, http://dx.doi.org/10.1016/j.jcp.2018.01.022.
[39] C. Barus, Isothermal, isopiestics and isometric relative to viscosity, Am. J. Sci. 45 (266) (1893) 87–96, http://dx.doi.org/10.2475/ajs.s3-45.266.87.
[40] L. Franca, R. Stenberg, Error analysis of Galerkin least squares methods for the elasticity equations, SIAM J. Numer. Anal. 28 (6) (1991) 1680–1697, http://dx.doi.org/10.1137/0728084.
[41] G. Barrenechea, F. Valentin, An unusual stabilized finite element method for a generalized Stokes problem, Numer. Math. 92 (4) (2002) 653–677, http://dx.doi.org/10.1007/s002110100371.
[42] D. Boffi, F. Brezzi, M. Fortin, Mixed Finite Element Methods and Applications, Springer Series in Computational Mathematics, vol. 44, Springer Berlin Heidelberg, 2013, http://dx.doi.org/10.1007/978-3-642-36519-5.
[43] A. Ern, J.-L. Guermond, Theory and Practice of Finite Elements, Applied Mathematical Sciences, vol. 159, Springer-Verlag, New York, 2004, http://dx.doi.org/10.1007/978-1-4757-4355-5.
[44] S. Agmon, Lectures on Elliptic Boundary Value Problems, AMS Chelsea Publishing, Providence, RI, 2010, http://dx.doi.org/10.1090/chel/369.
[45] S.C. Brenner, L.R. Scott, The Mathematical Theory of Finite Element Methods, third ed., Texts in Applied Mathematics, vol. 15, Springer, New York, 2008, http://dx.doi.org/10.1007/978-0-387-75934-0.
[46] J. Cheung, M. Perego, P. Bochev, M. Gunzburger, Optimally accurate higher-order finite element methods for polytopial approximations of domains with smooth boundaries, Math. Comp. 88 (319) (2019) 2187–2219, http://dx.doi.org/10.1090/mcom/3415.
[47] S. Prössdorf, B. Silbermann, Numerical Analysis for Integral and Related Operator Equations, Operator Theory: Advances and Applications, vol. 52, Birkhäuser Verlag, Basel, 1991, p. 542.
[48] A. Logg, G. Wells, K. Mardal (Eds.), Automated solution of differential equations by the finite element method. The FEniCS book, Lecture Notes in Computational Science and Engineering, vol. 84, Springer-Verlag Berlin Heidelberg, 2012, http://dx.doi.org/10.1007/978-3-642-23099-8.
[49] P. Clément, Approximation by finite element functions using local regularization, RAIRO Anal. Numer. 9 (1975) 77–84, http://dx.doi.org/10.1051/m2an/197509R200771.